


## Article

# Updated Virophage Taxonomy and Distinction from Polinton-like Viruses

Simon Roux <sup>1,\*</sup> , Matthias G. Fischer <sup>2</sup> , Thomas Hackl <sup>3</sup> , Laura A. Katz <sup>4</sup> , Frederik Schulz <sup>1</sup>   
and Natalya Yutin <sup>5</sup>

<sup>1</sup> DOE Joint Genome Institute, Lawrence Berkeley National Laboratory, Berkeley, CA 94720, USA

<sup>2</sup> Max Planck Institute for Medical Research, Department of Biomolecular Mechanisms, 69120 Heidelberg, Germany

<sup>3</sup> Groningen Institute of Evolutionary Life Sciences, University of Groningen, 9700 AB Groningen, The Netherlands

<sup>4</sup> Department of Biological Sciences, Smith College, Northampton, MA 01063, USA

<sup>5</sup> National Center for Biotechnology Information, National Library of Medicine, National Institutes of Health, Bethesda, MD 20894, USA

\* Correspondence: sroux@lbl.gov

**Abstract:** Virophages are small dsDNA viruses that hijack the machinery of giant viruses during the co-infection of a protist (i.e., microeukaryotic) host and represent an exceptional case of “hyperparasitism” in the viral world. While only a handful of virophages have been isolated, a vast diversity of virophage-like sequences have been uncovered from diverse metagenomes. Their wide ecological distribution, idiosyncratic infection and replication strategy, ability to integrate into protist and giant virus genomes and potential role in antiviral defense have made virophages a topic of broad interest. However, one limitation for further studies is the lack of clarity regarding the nomenclature and taxonomy of this group of viruses. Specifically, virophages have been linked in the literature to other “virophage-like” mobile genetic elements and viruses, including polinton-like viruses (PLVs), but there are no formal demarcation criteria and proper nomenclature for either group, i.e., virophage or PLVs. Here, as part of the ICTV Virophage Study Group, we leverage a large set of genomes gathered from published datasets as well as newly generated protist genomes to propose delineation criteria and classification methods at multiple taxonomic ranks for virophages ‘sensu stricto’, i.e., genomes related to the prototype isolates Sputnik and mavirus. Based on a combination of comparative genomics and phylogenetic analyses, we show that this group of virophages forms a cohesive taxon that we propose to establish at the class level and suggest a subdivision into four orders and seven families with distinctive ecogenomic features. Finally, to illustrate how the proposed delineation criteria and classification method would be used, we apply these to two recently published datasets, which we show include both virophages and other virophage-related elements. Overall, we see this proposed classification as a necessary first step to provide a robust taxonomic framework in this area of the virosphere, which will need to be expanded in the future to cover other virophage-related viruses such as PLVs.

**Keywords:** virophage; polinton; polintovirus; giant virus; virus taxonomy



**Citation:** Roux, S.; Fischer, M.G.; Hackl, T.; Katz, L.A.; Schulz, F.; Yutin, N. Updated Virophage Taxonomy and Distinction from Polinton-like Viruses. *Biomolecules* **2023**, *13*, 204. <https://doi.org/10.3390/biom13020204>

Academic Editors: Eugene V. Koonin and Oxana V. Galzitskaya

Received: 28 November 2022

Revised: 2 January 2023

Accepted: 4 January 2023

Published: 19 January 2023



**Copyright:** © 2023 by the authors. Licensee MDPI, Basel, Switzerland. This article is an open access article distributed under the terms and conditions of the Creative Commons Attribution (CC BY) license (<https://creativecommons.org/licenses/by/4.0/>).

## 1. Introduction

“Virophage” is a generic term currently used to describe viruses with dsDNA genomes that are able to co-infect a eukaryotic cell alongside a giant virus and then hijack parts of the giant virus machinery for their own replication [1–3]. The first virophage was discovered in an amoeba host (*Acanthamoeba castellanii*) alongside the giant Mamavirus and was named Sputnik because of its satellite-like reliance on the Mamavirus machinery [4]. A second virophage, named mavirus, was characterized soon after [5]. It was found co-infecting the marine flagellate *Cafeteria* sp. with the giant *Cafeteria roenbergensis* virus (CroV) and

revealed an evolutionary link between virophages and eukaryotic mobile genetic elements of the *Maverick/Polinton* class. A handful of additional virophages have been cultivated and characterized since, including multiple Sputnik-like and Zamilon virophages associated with different mimivirus strains, and more recently, the first virophage of a green alga, *Chlorella* virus virophage SW01 (CVv-SW01), which depends on the CroV-like *Chlorella* Virus XW01 [2,6,7]. For clarity, the term “virophage” will be used hereafter to designate specifically viruses related to Sputnik, Zamilon, mavirus, and CVv-SW01.

Comparative analysis of isolated virophages outlined several genomic and phenotypic defining characteristics. Their double-stranded (ds) DNA genomes are around 20 kilobases (kb) long, feature a low GC content, and encode for  $\approx 20$  predicted proteins [2,8]. Their major capsid protein adopts a double jelly-roll (DJR) fold and forms the shell of a 50 to 75 nm-wide icosahedral virion. In addition to recognizable structural genes (e.g., major and minor capsid proteins), all virophages encode two other proteins likely involved in encapsidation, an Adenain-like maturation protease, and an FtsK-HerA-like ATPase. Finally, these virophages only replicate when their protist host is co-infected with a giant virus, specifically from the *Imitervirales* order. The extent of the negative effect of virophage replication on the giant virus replication and burst size varies, as co-infection results in severe inhibition of the giant virus in the case of Sputnik and mavirus, but not for Zamilon [3]. These defining characteristics were the basis for the initial taxonomic classification of virophages, proposed in 2016 [9]. Briefly, one family (*Lavidaviridae*) and two genera (*Sputnikvirus* and *Mavirus*) were established to include the three recognized dsDNA virophage species at the time: *Cafeteriavirus-dependent mavirus*, *Mimivirus-dependent virus Sputnik*, and *Mimivirus-dependent virus Zamilon*. This taxonomy was amended in 2020 with the addition of higher ranks that connected existing virophage taxa to the larger *Preplasmiviricota* phylum, *Bamfordvirae* kingdom, and *Varidnaviria* realm [10].

The characterization of Sputnik and mavirus also enabled large-scale searches for virophage-like sequences in metagenomes, which uncovered a broad diversity of virophages existing in the environment. Virophage-like sequences were detected across many types of biomes, including human and other animal gut microbiomes [11,12], as well as freshwater lakes from Antarctica [13], North America [14–16], Asia [17,18], and Europe [19]. Further comparative genomic studies, including a large compendium of genomes assembled from metagenomes, indicated that these virophage (-like) sequences were diverse and part of a larger evolutionary network including other eukaryotic viruses & mobile genetic elements, most notably polinton-like viruses (PLVs) [19–23]. Like virophages, PLVs seem to be evolutionary related to mobile genetic elements of the *Maverick/Polinton* class, can co-infect eukaryotic host cells alongside a giant virus, and seemingly encode a comparable encapsidation machinery although with no detectable sequence similarity to the one of virophages [24–26]. Meanwhile, the integration of mavirus-like virophages into their eukaryotic host genomes and subsequent reactivation was further explored and revealed a high degree of mobility, with a potential role as a population-based defense system against their cognate giant viruses [27,28]. The unexpected plethora of virophage-like elements revealed by these different studies resulted in a confusing nomenclature where different labels were given for entities that had similar or overlapping properties. Specifically, virophage-related sequences were alternatively reported as “virophages,” “polintons,” “polintonviruses,” “polinton-like viruses,” “adintoviruses,” or “MELD viruses” [19,23,24,29]. The use of different names reflects the current lack of a taxonomic framework for virophages and related elements, owing to the fast increase of metagenomic sequence reports in recent years.

Here, in support of the ICTV virophage study group, we reanalyze a comprehensive set of virophage-like metagenome-derived genomes complemented with additional host-associated datasets to provide a unified identification and classification framework. Specifically, we first update the virophage taxon demarcation criteria to be applicable to uncultivated virophages, then we evaluate how phylogenetic and gene content analyses can be combined to identify robust clades within this virophage taxon, and finally, we

explore how these metagenome-derived sequences, taken together, inform on the ecological distribution and host range of virophages.

## 2. Results & Discussion

### 2.1. Definition of a Formal Virophage Taxon and Associated Demarcation Criteria

To be operationally useful for metagenome-derived sequences, taxon delineation criteria should be based on genome features only and complemented by additional information if/when available. The current official demarcation criteria of the *Lavidaviridae* family, to which all virophages belong, include both genetic markers and phenotypic information (a virus that is “dependent on or associated with, a large dsDNA virus related to the so-called nucleo-cytoplasmic large DNA viruses”) [9,10]. The genetic markers criteria highlighted four genes from the morphogenetic module that were shared by all known virophages and can be used in phylogenetic analysis to demonstrate genetic similarity and common origin. These four genes include virophage-specific versions of (i) major capsid protein (MCP), also known as “hexon” protein, (ii) minor capsid protein (minCP), also known as “penton” protein, (iii) FtsK-HerA family DNA-packaging ATPase (ATPase), and (iv) maturation cysteine protease (PRO), also known as Adenain. Since these demarcation criteria were first proposed, several studies confirmed the co-occurrence of MCP, ATPase, and PRO in complete or near-complete genomes [6,12]. The virophage penton protein is also most often detected, with some rare exceptions where it seems to have diverged beyond recognition, as in the rumen virophages (RMV) [11].

To confirm whether gene content alone could be used to distinguish virophages such as Sputnik and mavirus from other related elements, we first searched the 36 sequences currently assigned to the *Lavidaviridae* family in GenBank and the largest RMV sequence using HMM profiles previously established for each of these marker genes [12]. Most lavidavirus genomes included the four virophage marker genes, with the known exception of RMVs lacking an identifiable virophage-like penton protein (Figure 1). Four genomes encoded none of these markers, namely *Phaeocystis globosa* virus virophage and three *Chrysochromulina parva* virus virophages. These genomes were already known to be more similar to polinton-like viruses and thus would logically not belong to the same taxon as other virophages [11]; however, they provide a good opportunity to formally define the new taxon boundaries. Specifically, no gene of these polinton-like viruses showed significant similarity to any of the virophage marker genes (highest hmmsearch scores < 10), while virophage sequences typically displayed hmmsearch scores  $\geq 100$ , except for the penton protein (Figure 1B). We thus propose to update the delineation criteria for a virophage taxon as follows:

- required features: the complete genome should encode a virophage-like hexon protein, a virophage-like ATPase, and a virophage-like cysteine protease, all of which can be detected based on established HMM profiles for each of these marker genes
- other expected (but not required) features: the genome should consist of dsDNA with a length between 15 kb and 45 kb and encode a virophage-like penton protein detected based on established HMM profile(s).

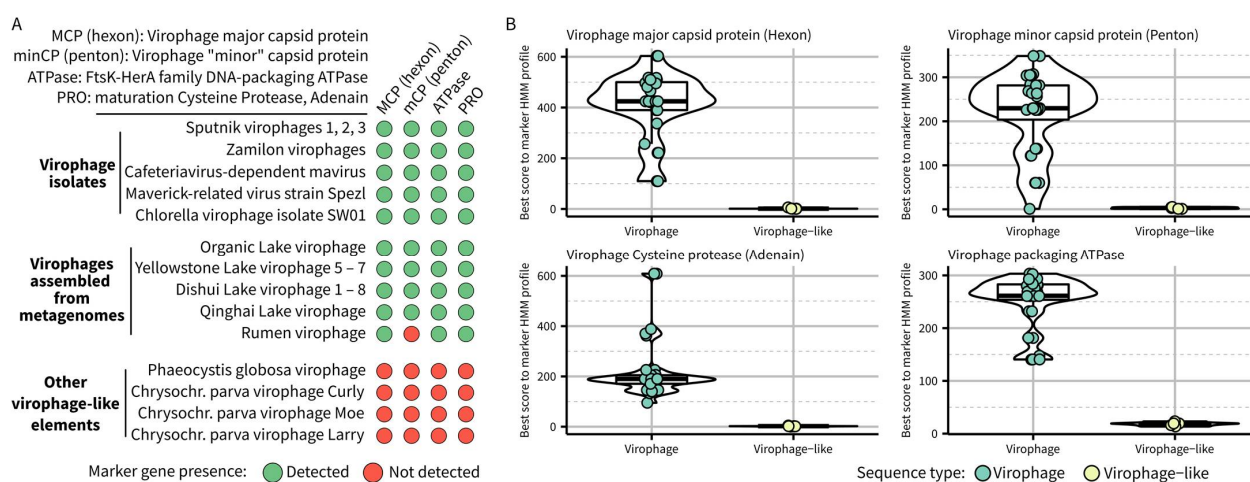


**Figure 1.** Detection of virophage marker genes across sequences currently classified in the *Lavidaviridae* family on GenBank. Marker genes were detected based on an hmmsearch performed between predicted proteins from the *Lavidaviridae* genomes and HMM profiles previously built for the four conserved genes in the virophage morphogenesis gene module [12]. Panel (A) displays the pattern of conserved gene detection for virophage isolates, virophage genomes assembled from metagenomes, and virophage-like elements currently classified as *Lavidaviridae* on GenBank but not encoding any of the virophage conserved genes. Panel (B) displays the distribution of the hmmsearch score for each marker for both the virophages (isolates or assembled from metagenomes) and the virophage-like elements. Accession numbers for the different genomes used here are indicated in Table S1.

## 2.2. Common Origin and Genetic Diversity in the Extant Virophage Clade

To explore the genetic diversity within the virophage clade as defined by the demarcation criteria above, we used the same HMM profiles of the four virophage marker genes to gather virophage sequences from previously published datasets [12,28,30], public databases (as of October 2021), and newly-sequenced protist genomes (Table S1). Specifically, we retained all sequences for which at least three of the four virophage marker genes could be detected. The resulting 1869 sequences were clustered into 848 distinct viral operational taxonomic units (vOTUs) using standard cutoffs for dsDNA viruses, i.e., 95% average nucleotide identity (ANI) and 85% alignment fraction (AF) [31]. Among these, 257 vOTU representatives were predicted to be complete or near-complete (Figure S1, Table S1, and see Section 4. Methods). All 257 (near)-complete genomes encoded the MCP and ATPase genes, 256 encoded a PRO gene, and 247 also encoded a recognizable penton protein (minCP), confirming that virophages typically encode all 4 of these marker genes.

We first used this dataset in phylogenetic analyses to confirm that virophages form a cohesive taxon (Figure S2). In trees built from the ATPase and PRO genes, the two markers for which alignable homologs can be identified in other viruses and/or cellular genomes, all virophage sequences formed a monophyletic group (Figure S2). The only exception was an ATPase encoded on a contig from a Pithovirus MAG (LCPAC001) that branched within the virophage clade and may be a genuine virophage erroneously binned in a giant virus genome (see below). Overall, these two rooted trees confirmed that virophages could be classified as a single monophyletic taxon and reinforced the use of the four marker genes for virophage classification.

Next, we performed de novo protein clustering to estimate the diversity of genes encoded in virophage genomes. This clustering highlighted the four marker genes from the morphogenesis gene module as the only near-universally conserved ones in the dataset. No other genes were identified in more than half of the genomes, even when using sensitive clustering approaches (Figure 2A). Specifically, each (near)-complete virophage genome encodes, on average, 27 predicted proteins with a majority either unique to a single vOTU ( $n = 6$ ) or detected in less than 10% of virophage vOTUs ( $n = 8$ ), highlighting the high level of divergence between virophage genomes. A similar pattern can be observed when

analyzing pairwise similarity for the morphogenesis genes: while each gene can readily be identified via key conserved residues, most virophone pairs show less than 30% amino-acid sequence similarity in their MCP, minCP, PRO, or ATPase (Figure 2B). Taken together, the low similarity in primary sequence, even for conserved genes, coupled with the high diversity in other genes indicates that, despite their likely common origin and recognizable set of conserved genes, virophone genomes encode a large and mostly idiosyncratic genetic diversity. We propose that this level of diversity justifies the establishment of a taxon at the class level, i.e., *Maveriviricetes*. The demarcation criteria listed above should thus be interpreted as defining whether a virus belongs to the *Maveriviricetes* class.

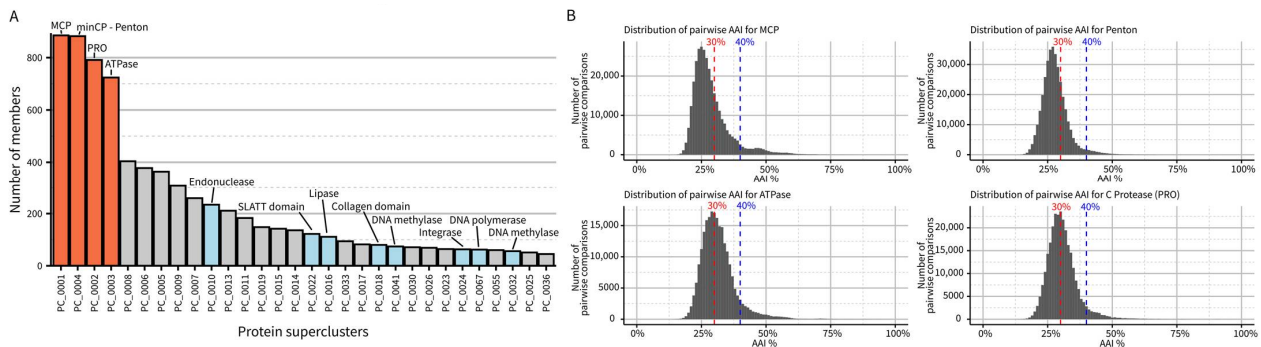


**Figure 2.** Genetic diversity in virophone genomes. **(A)** Size distribution and functional annotation of the 30 largest protein clusters obtained from the virophone sequences. The four conserved genes are colored in orange, while other protein clusters functionally annotated are colored in blue. **(B)** Distribution of pairwise amino-acid identity (AAI) across all virophone sequences for the four conserved morphogenesis genes. Two standard AAI cutoffs (30% and 40% AAI) are highlighted in red and blue, respectively. MCP: Major Capsid Protein (hexon). Penton: minor capsid protein.

### 2.3. Challenges and Limitations of Taxonomic Classification within the Virophone Clade

As illustrated above by the diverse gene content and low level of similarity even for conserved genes, establishing robust lower-level taxa within the virophone clade, i.e., within the *Maveriviricetes* class, is challenging. The current ICTV taxonomy defines one genus each for *Sputnik* and *Mavirus* virophone species, which is not sufficient to handle the additional diversity described. Here, we explored whether consistent clades can be derived from a phylogeny based on MCP, the most conserved gene across virophages, and gene content clustering based on genome-wide amino acid identity (gwAAI). This analysis was restricted to the set of 257 virophone genomes identified as complete or near-complete (see above).

The major capsid protein (MCP) was selected for phylogeny reconstruction as it was the longest of the four genes in the morphogenesis gene module (Figure S3). Consistent with previous studies, the MCP phylogeny was difficult to resolve due to high sequence divergence, and the resulting tree included some long branches with uncertain placement. Nevertheless, for most of the tree, robust monophyletic clades with strong (>90) bootstrap support can be delineated and used to form the basis of formal taxa (Figure 3A). To identify which clades were the most appropriate to define as taxa, we added complementary information, including genome features (genome length, MCP length, presence of a recognizable penton), clustering based on gwAAI, and source environment, to the MCP tree, with the rationale that any taxon should ideally have distinguishing characteristics beyond grouping in a monophyletic clade in the tree (Figure 3A).

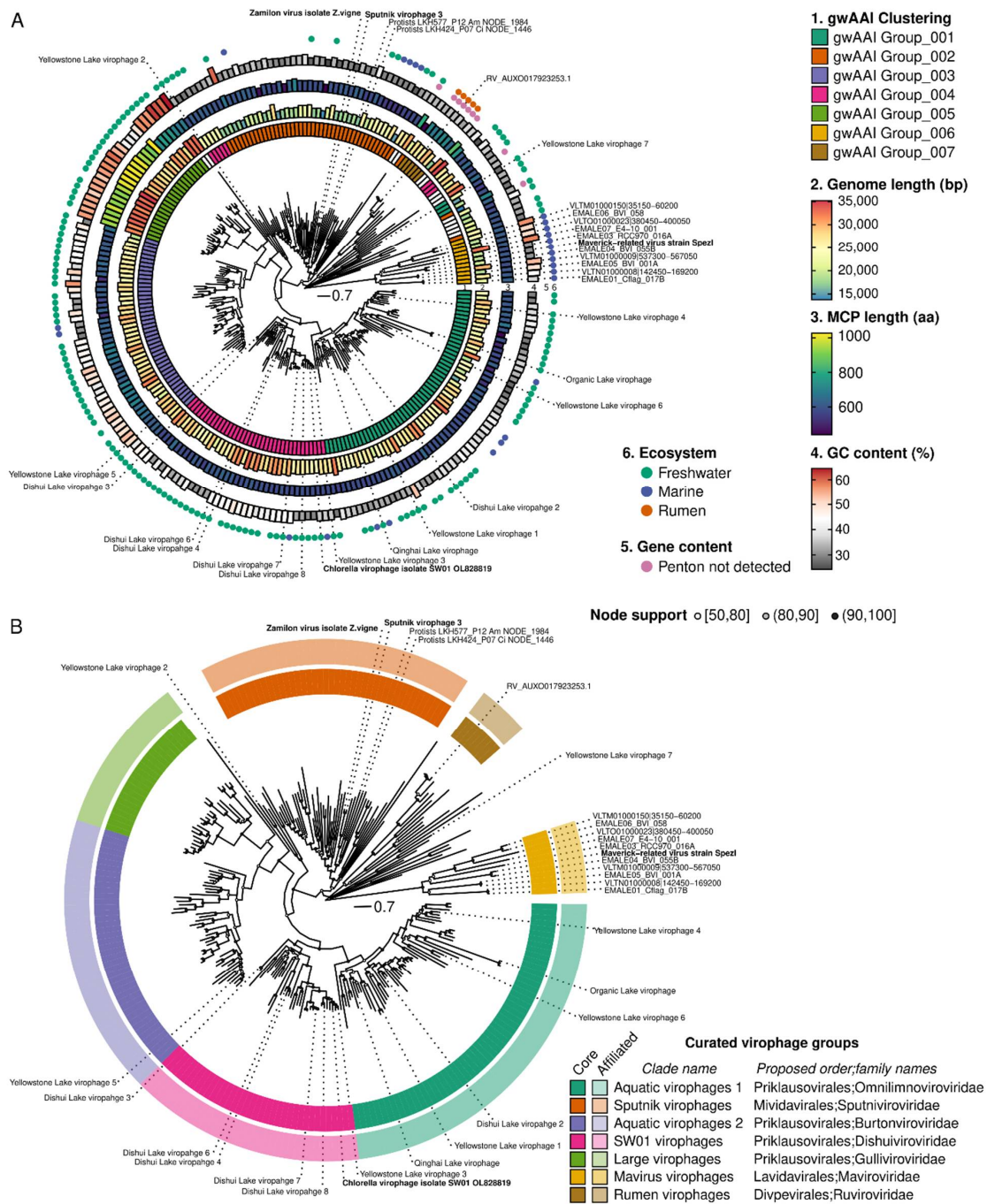


**Figure 3.** Definition of new virophage clades based on MCP phylogeny and genome features. For both panels, an MCP phylogeny is presented based on complete and near-complete virophage genomes. For panel (A), genomes features are displayed including from the inner to the outer ring: (1) groups based on genome-wide amino-acid identity (gwAAI) considering the seven largest groups, (2) genome length, (3) Major Capsid Protein (MCP) length, (4) average GC content, (5) detection of the typical virophage penton protein based on HMM profiles, and (6) ecosystem from which the genome was obtained. In panel (B), the same tree is decorated with the classification of virophage genomes in curated groups. The “core” sequences (solid colors, inner ring) of each group represent the members of the monophyletic clade assigned to this group based on the gwAAI clustering (see panel (A)). The “affiliated” ring displays the results of a “best BLAST hit” affiliation of all sequences in the tree (ignoring self-hits) in light colors (outer ring).

Combining phylogeny and genome metadata enabled us to delineate seven distinct groups within this dataset (Figure 3A,B). The first one noted as “mavirus virophage” in Figure 3B, represents virophages branching next to the mavirus isolate and clustered in the same group (“gwAAI Group\_006”) based on gwAAI. It includes 11 genomes, is only distantly related to other virophages on the MCP tree, and is mostly composed of sequences integrated into *Cafeteria* genomes. Similarly, a small group noted as “Rumen virophage” is composed of 6 genomes clustered in the same gwAAI group (“gwAAI Group\_007”) and only distantly related to other virophages on the MCP tree. This second group includes the sequences originally described as “rumen virophages” [11], along with other metagenome-derived, genomes mostly from rumen samples (Figure 3A and Figure S4). The third group (“Sputnik virophages”) is formed by a monophyletic clade of 47 genomes, including Zamilon and Sputnik virophages, the majority (all but 2) clustered in “AAI Group\_002”. This group also displays short genomes (median = 18.9 kb) and a relatively low GC content (median = 31.3%) compared to other virophages (Figure S4). The fourth group noted as “large virophage,” forms a distinct clade with characteristically large genomes (median = 31.4 kb) and MCPs (median length = 938 aa), as well as unusually high GC content (median = 55.2%, Figure 3A and Figure S4). Finally, three groups noted as “SW01 virophages”, “aquatic virophages 1”, and “aquatic virophages 2,” include 146 genomes branching next to the “large virophages” but displaying genome lengths, MCP lengths, and GC content comparable to other virophages, and clustered into three distinct gwAAI groups (Figure 3A,B and Figure S4). The former (“SW01 virophages”) includes the recently isolated *Chlorella* virophage SW01, while the other two lack an isolated representative [6].

In addition to forming monophyletic clades on an MCP tree, we further verified whether members of these groups also formed monophyletic clades on trees built from the three other virophage morphogenesis genes. The divergence level for these markers led to sub-optimal alignments and consistently long branches so that the deeper structure of the trees remained uncertain. Nevertheless, all clades remain broadly monophyletic on the ATPase and penton trees, with only a handful of inconsistent sequences (Figure S5). In the PRO tree, rumen virophages branched within SW01 virophages, and mavirus virophages branched within Sputnik virophages, but both rumen and mavirus virophages were associated with long branches and lower node support (often < 80). This suggests that, while clades overall remained consistent across markers, their relative position to one another is challenging to resolve, given the level of diversity in the different alignments. This is also true for the MCP tree, where some genomes display long branches that cannot be placed with certainty (e.g., Yellowstone Lake virophage 7).

Given the robustness of the seven delineated clades, and as part of the ICTV virophage sub-group, we will propose to establish these as formal taxa at the order and family level, as follows:

- Rumen virophages as the new *Ruviroviridae* family in the new *Diopevirales* order, named for virophages with Divergent penton proteins.
- Mavirus virophages as the new *Maviroviridae* family after the first isolated member of the taxon, in the new *Lavidavirales* order, a name adapted from the current *Lavidaviridae* family named for “Large virus dependent or associated.”
- Sputnik virophages as the new *Sputniviroviridae* family after the first isolated member of the taxon, in the new *Mividavirales* order, for “Mimivirus dependent or associated”
- SW01 virophages as the new *Dishuiviroviridae* family after the lake from which the first member of the taxon (SW01) was isolated, in the *Priklausovirales* order, which is currently the only order established in the *Maveriviricetes* class.
- Aquatic virophages 1 as the new *Omnilimnoviroviridae* family using the prefixes “omni” (“all,” “everywhere”) and “limno” denoting a link to freshwater environments, since members of this clade were detected across a broad geographic range of freshwater lakes, also in the same *Priklausovirales* order.
- Large virophages as the new *Gulliviroviridae* family named after Lemuel Gulliver, the main character of “Gulliver’s travel,” since these virophages can be considered as

“giant” compared to other virophages but are still relatively small compared to their associated giant viruses, also in the same *Priklausovirales* order.

- Aquatic virophages 2 as the new *Burtonviroviridae* family named after Mary Burton, the wife of Lemuel Gulliver in “Gulliver’s travel,” as this clade is the most closely related to the large virophages, also in the same *Priklausovirales* order.

The decision to group the latter four clades in a single order (*Priklausovirales*), and separate all others, was based on the divergence between clades observed in the tree and the pairwise MCP AAI (Figure S4G).

#### 2.4. Examples of Detection and Taxonomic Assignment of Virophages in Mixed Datasets

Building on this new framework, the next step was to establish criteria and operational processes to assign new sequences to these virophage taxa. Ideally, new virophage sequences would be classified based on similar approaches as the ones used above to delineate taxa, i.e., combining multiple phylogenies, genome features, and genome-wide AAI clustering. We recognize, however, that this approach may be impractical in some cases, and an alternative method to assign new sequences to existing virophage taxa based on a simple sequence comparison to reference profiles or databases would be valuable. Based on the new proposed taxa and demarcation criteria outlined above, we built and benchmarked such an approach and provided it as an integrated package including relevant databases and an automated classifier (Figure 4A, [https://github.com/simroux/ICTV\\_VirophageSG](https://github.com/simroux/ICTV_VirophageSG), accessed on 15 November 2022).

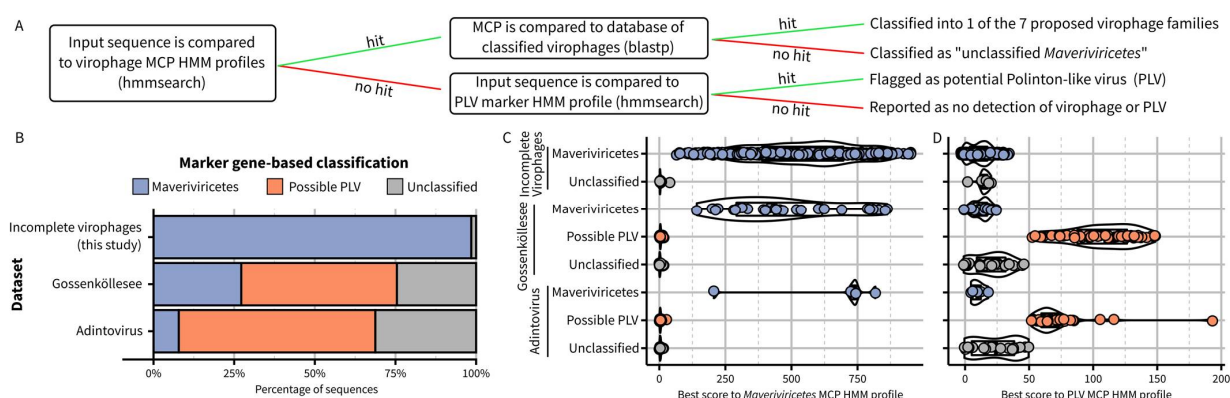


**Figure 4.** Detection and classification of virophages from published datasets. (A) Schematic overview of the hmmsearch- and BLAST-based classification approach used to identify and assign virophages to the proposed families. For panels (B–D), three datasets were processed with the approach described in panel (A). The first includes non-redundant previously published virophage sequences gathered as part of this study and not included in the complete and near-complete genome set ( $n = 591$ ; “Incomplete virophages”). The second includes contigs identified as virophages and Polinton-like viruses assembled from Gossenköllesee metagenomes and published in [19] ( $n = 114$ ; “Gossenköllesee”). Finally, the third dataset included adintoviruses published in several previous studies [23,32,33] ( $n = 64$ ; “Adintovirus”). In panel (B), the percentage of sequences assigned as *Maveriviricetes* (based on MCP HMM) or with a hit to the PLV HMM profile is indicated. The score distribution of score for the hits to the *Maveriviricetes* HMM or PLV HMM is displayed in panels (C,D), respectively, for each dataset and each group of sequence.

To determine whether a new sequence belongs to the *Maveriviricetes* class as defined above, we built updated HMM profiles for each of the four morphogenesis genes and specifically recommend using the detection of the MCP profile as the main demarcation criteria, with the three other markers primarily used to confirm this assignment and providing a measure of genome completeness. Within *Maveriviricetes*, we propose assigning new sequences to the seven taxa using a best BlastP hit approach to MCP references, with cutoffs derived from comparing complete and near-complete genomes (Figure 4A,



Table S2). This “best hit” approach was selected rather than a clustering based on MCP pairwise AAI due to the limited ability of the latter to distinguish “within taxa” from “between taxa” comparisons (Figure S4G). When applied to the set of reference sequences and omitting self-hits, BLAST-based affiliations recapitulated the classification of all original members of each family defined based on the MCP phylogeny (Figure 3B). Hence, while not strictly identical, this BLAST-based assignment should be a useful approximation to the phylogeny-driven families defined above. Finally, to help further distinguish between virophages within the *Maveriviricetes* class and Polinton-like viruses (PLVs), we included in the classifier a comparison to a previously published HMM profile corresponding to an FtsK-HerA ATPase conserved across PLVs [12,26]. Sequences not assigned to *Maveriviricetes* can thus be flagged as possible PLVs based on the detection of this profile (Figure 4A).

To illustrate how the process would work in practice, we first applied this BLAST-based assignment to the partial sequences in our dataset, i.e., virophage sequences that were not identified as complete or near-complete and thus not included in the main MCP phylogeny. Overall, 393 (66%) of these sequences could be assigned at the family level, with the majority classified in the new Burtonviroviridae proposed family (31% of the assigned sequences, Table S3). As further confirmation, we performed a phylogeny-based affiliation for these same sequences, which was nearly identical to the BLAST-based approach (92% of sequences with identical assignment, Figure S6). We next applied the BLAST-based assignment approach to a dataset obtained from a high-altitude mountain lake in which virophage-like sequences had been previously identified via a custom gene content approach [19]. Overall, 31 sequences were classified in the *Maveriviricetes* class based on the detection of a virophage MCP, including 26 for which all four marker genes could be detected and another three for which three of the four marker genes could be detected (Figure 4A, Table S3). These 31 sequences corresponded almost exactly to the list of 32 virophages highlighted in the original study, with the only one sequence missing being a partial genome in which no MCP was detected. We also applied the same approach to previously published “Adintoviruses” (n = 64), of which several were classified as *Polintoviricetes*, another class next to the *Maveriviricetes* within the *Preplasmiviricota* phylum [23,32,33]. Among these, five sequences were classified as *Maveriviricetes* with our approach, all displaying three or four of the virophage morphogenesis genes. Genome comparison further confirmed that four of these sequences were similar to rumen virophages (n = 4), which would justify a reclassification in the *Maveriviricetes* taxon (Figure S7).

For the detection of PLVs, 53 of the 77 sequences that had been previously identified as “PLV” in the Gossenköllesee dataset displayed a hit to the PLV FtsK-HerA ATPase profile, while none of the virophages did (Figure 4B,C). Similarly, 39 of the 64 adintoviruses displayed a hit to this PLV profile, including the two ICTV-recognized exemplar genomes for the *Polintoviricetes* class: Mayetiola barley midge adintovirus strain 2012 and Terapene box turtle adintovirus isolate 5272. This suggests that the *Polintoviricetes* class may eventually serve as a formal taxon for most, if not all, PLVs. Notably, PgVV and the three *Chrysochromulina parva* virus virophages, which are currently classified in the *Lavidaviridae* in GenBank, do not fulfill the criteria described above for classification into the *Maveriviricetes* (Figure 1) and display a significant hit to this PLV profile, suggesting they should be reclassified into the *Polintoviricetes* class.

Finally, while identifying virophages in public databases, we noticed 12 contigs fulfilling all criteria for classification in *Maveriviricetes* but currently classified as Bacteria or Archaea (Table S1—abbreviated sequence ids starting with “MAG\_”). All these contigs originated from metagenome-assembled genomes (MAGs) and likely reflected erroneous binning. This indicates that virophage contigs represent an underestimated source of prokaryotic MAG contamination, which may stay undetected by current tools.

### 2.5. Beyond Genome-Based Taxonomy: Virophage Host Range and Interactions

A better characterization of virophage and virophage-like evolutionary history and taxonomy is especially important to better understand the impact and long-term association

of these elements with their giant virus and eukaryotic hosts. Both Sputnik and mavirus hijack the molecular machinery of their associated giant viruses and, in so doing, likely reduce the burden imposed on the protist host community by these eukaryotic viruses. A recent PLV-like element showed a similar association with both a giant virus and a eukaryotic virus and a reduction in the fitness of the giant virus, suggesting this lifestyle and infection cycle may be a common feature of virophages and PLVs [25]. However, most virophages are only known from metagenome assemblies; thus we lack information about their potential giant virus and eukaryotic hosts. Mining eukaryotic genomes, either from isolates or obtained through single-cell genomics, can help bridge this gap.

Our virophage dataset included 36 sequences identified in eukaryotic genomes obtained from cultivated strains. A majority (34 of 36) were detected in *Cafeteria burkhardae* (formerly *C. roenbergensis*) genomes, including 11 integrated into a larger host region, as previously reported [28]. Notably, three metagenome-derived virophage genomes were similarly identified on larger contigs, including a likely host region of 5 to 10 kb (Table S1). While these host regions are similar to various protist taxa and do not allow a clear host prediction for these virophages, they suggest that additional instances of virophage integration could be discovered from metagenomes in the near future. The two other virophages detected in eukaryotic genomes were detected in the genomes of *Caecitellus* and an *Adriamonas*-like bicosoecid, marine, and freshwater heterotrophic flagellates, respectively (Table S4; Hackl, Arndt, Fischer, unpublished). According to the BLAST-based approach (see above), the former was classified as an aquatic virophage group 2 (proposed Burtonviroviridae), while the latter remained unclassified within the *Maveriviricetes* class.

Since microeukaryotes are difficult to cultivate, however, single-cell genomics provides an alternative option to obtain genome sequences for individual microeukaryote cells either automatically sorted or handpicked from environmental samples. Our virophage dataset included 32 sequences obtained from partially sequenced single-cell genomes, providing additional indications of the type of eukaryotic hosts found across virophage diversity (Tables S1 and S4; Katz Lab, unpublished). These 32 sequences originated from eight genomes of the testate amoeba *Hyalosphenia elegans* (n = 16), six genomes from *Loxodes* spp. (n = 13), and two genomes from *Halteria* spp. (n = 3). Virophages classified in the proposed Sputnikviroviridae, Dishuiviroviridae, Omnilimnoviroviridae, and Burtonviroviridae families were identified, with some single-cell genomes including multiple distinct virophages suggesting the potential for co-infection. While these data point to additional hosts of virophages, such associations would have to be confirmed experimentally, as virophages could also be detected in single-cell genomes if they were attached to or engulfed in but not infecting the protist cell. Building on these candidate associations, further characterization of virophage-host interaction would ideally be performed using recently developed in vitro assays such as virusFISH [34] and droplet digital PCR [35].

### 3. Conclusions

Virophages are part of a fascinating and complex network of smaller dsDNA viruses that are associated with giant viruses and eukaryotic hosts. Based on metagenome analysis, virophages are a diverse group of viruses with a complex evolutionary history, which led to confusion regarding the extent, nomenclature, and characteristics of virophages as a taxonomic clade. As members of the ICTV virophage study group, we focused here on sequences similar to the virophages *stricto sensu* and sought to establish updated demarcation criteria that can be applied to both cultivated and uncultivated virophages. We then attempted to delineate robust taxa within this virophage clade based on the recently published datasets of metagenome-derived virophage genomes. This led us to propose that virophages, i.e., viruses similar to Sputnik and mavirus, should be placed in the *Maveriviricetes* clade and delineated based primarily on the double jelly-roll major capsid protein version that is unique to this clade, and on three other morphogenesis genes (minCP, ATPase, PRO) typically also encoded on these genomes. Within this class, we further propose to distinguish seven family-level groups, to be soon formally pro-

posed to ICTV, delineated based on a combination of phylogenetic and genome clustering approaches. Finally, we provide sequence-similarity-based approaches to assign newly sequenced virophages to these different groups. A similar framework could likely be used for PLVs, some of them currently classified in the *Polintoviricetes*, which would further clarify taxonomic classification in this area of the virosphere. There is much that remains to be discovered and characterized in terms of virophage and PLV biology, including host range, interaction with giant viruses and eukaryotic hosts, or potential new defense/counter-defense systems [25,36]. Ultimately, a comprehensive genome catalog of virophages, along with a clear and updated taxonomic scheme, represents a framework that will facilitate future studies and more in-depth characterization of these fascinating viruses.

## 4. Methods

### 4.1. Collection of Virophage and Virophage-Like Sequences

Virophage and virophage-like genomes used in this study (Table S1) were collected from multiple sources. First, all genomes classified as *Lavidaviridae* in the NCBI Nucleotide database were downloaded in March 2022, excluding partial genomes MN151334 and KJ183141, which only include a portion of the major capsid protein. This *Lavidaviridae* genome reference dataset (n = 28) also included sequences downloaded in 2014 from NCBI Nucleotide, namely Yellowstone Lake virophages 1 to 4 and Ace Lake virophage. Next, all sequences assigned as *Lavidaviridae* in IMG/VR v3 [30] were collected (n = 1417), as well as a large set of metagenome-derived virophage sequences published in 2019 and partially overlapping with IMG/VR v3 [12] (n = 331), and a set of unique virophage sequences described in 2015 from rumen samples [11] (n = 7). Finally, we included a set of recently described integrated virophages from *Cafeteria burkhardae* [28] (“EMALEs,” n = 6). All these sequences were verified to encode at least three of the four members of the virophage morphogenesis module, previously highlighted as identification criteria for members of the *Lavidaviridae* family [9]. This identification was based on published HMM profiles [12], searched with hmmsearch v3.3.2 [37] using a maximum E-value of 0.01 and a minimum score of 40. For all metagenome sequences, ecosystem information was derived from the Gold database [38] or the annotation information available in NCBI RefSeq [39].

To complement these published virophages, we added two sets of newly detected virophage sequences. First, we used published virophage major capsid protein (MCP) sequences in a BlastP search against the NCBI nr database (September 2021), identifying 96 putative virophages. After removing sequences identical to references previously collected and sequences not encoding at least three of the four conserved virophage genes (see above), a total of 46 additional virophage sequences were collected, including 28 detected in whole-genome sequencing of *Cafeteria burkhardae* and overlapping with the “EMALEs” dataset [28], 13 belonging to bacterial and archaeal MAGs and likely resulting from erroneous genome binning, and five metagenome-derived virus genomes currently classified in the *Adintoviridae* family or the MELD group [23,32,33]. Finally, we also included in our dataset 34 virophage sequences, i.e., including at least three of the four conserved virophage genes identified in newly sequenced genomes from cultivated protists (n = 2) or single-cell genomes obtained by whole genome amplification from hand-picked amoeba and ciliates (n = 32). These virophage sequences were included as they may be uniquely associated with a potential host, which could eventually be used as part of a taxonomic classification. More information about these protist genomes is included in Table S4.

### 4.2. External Datasets Used to Illustrate Virophage Identification and Classification Approach

Two published datasets were used to illustrate the identification and classification approach proposed here because they had been presented as including virophage and other related viruses [19] or noticed to do so based on our search of NCBI nr database [23,32,33]. For the former dataset, identified as “Gossenköllesee,” all new contigs identified by the authors as virophages or PLV were downloaded from <https://figshare.com/s/9a7a1d16d77ea9d658a1>, accessed on 23 September 2022, and processed through the identification and

classification pipeline (n = 114). The original affiliation of these contigs was obtained from Table S3 in [19]. For the latter datasets, all contigs classified in the *Adintoviridae* family and available in NCBI GenBank in August 2022 were collected (n = 28) as well as the contigs listed in [23], which include additional unclassified viruses (n = 59). The two datasets were combined and dereplicated using MUMmer v4.0.0b2 [40] at 99% average nucleotide identity (ANI) over 99% of the shorter sequence length to obtain a non-redundant dataset of 64 sequences, referred to as “Adintovirus.”

#### 4.3. Virophage Genome Clustering, Quality Control, and Trimming

Sequences possibly corresponding to integrated virophages were first refined to trim any possible host region that may be found on the same contig. For all virophages detected in *Cafeteria burkhardae* genomes, a procedure similar to that of [28] was used. Briefly, for each virophage MCP, a region including 50 kb upstream and downstream was extracted. Predicted coding sequences (cds) in this region were compared to cds from the Mavirus reference genomes using BlastP 2.10.0+ [41] with a minimum bit score of 30. A custom script was used to calculate GC content on the same regions with 100 nucleotide sliding windows. Information was combined and individually inspected for each region to define the most likely boundaries of the integrated virophage, i.e., including known virophage genes and corresponding to a clear shift in GC content [28]. For metagenome sequences obtained from the IMG/VR database or the large previously published dataset [12], putative integrated virophages were identified as follows. First, all these contigs were screened for intergenic regions  $\geq 1$  kb, a common occurrence when annotating eukaryotic genomes with prokaryotic gene predictors (prodigal v2.6.3, “meta” option, see below). The 49 contigs with an intergenic region  $\geq 1$  kb were visually inspected on the IMG website to identify potential host regions. This led to the trimming of a potential host region for nine contigs (IMG\_VR\_0446, IMG\_VR\_0447, IMG\_VR\_0497, IMG\_VR\_0676, IMG\_VR\_0763, PE\_122, PE\_123, and PE\_131, Table S1). Second, contigs larger than 30 kb were searched for shifts in GC content, as observed in *Cafeteria burkhardae* genomes. This was observed for one contig (IMG\_VR\_0457), for which the host region was manually identified and trimmed (Table S1). For these metagenome-derived integrated virophages, cds predicted in the host region were compared to NCBI nr restricted to the Eukaryota taxon using online NCBI BLAST (August 2022) to determine a potential taxonomy for these host regions.

For contigs not identified as integrated proviruses, direct terminal repeats were detected based on identical sequences of at least ten nucleotides in 5' and 3' (n = 81). For all these contigs, all the duplicated sequence in 3' was trimmed to only retain a single genome unit. When needed, the start of the trimmed contig was shifted to avoid cds prediction spanning across the ends of the contig, leading to incomplete protein sequences.

All post-trimming virophage sequences (n = 1869) were next clustered into vOTUs following standard cutoff for dsDNA virus genomes, i.e., 95% ANI over 85% of the shortest sequence [31], using MUMmer v4.0.0b2 [40] to identify sequence similarity. The longest sequence was picked as the representative for each vOTU, except for ones including isolate and/or reference sequences, for which the oldest and/or highest quality reference genome was manually picked as the representative. The final dataset of 848 vOTU representatives, i.e., non-redundant virophage genomes, was used as input for subsequent analyses, including genome annotation, protein clustering, and phylogenies.

#### 4.4. Genome Annotation and De Novo Protein Clustering

For all trimmed representative sequences (see above), cds were predicted using prodigal v2.6.3 with the “meta” option [42]. For functional annotation, predicted protein sequences were then compared to the Pdb70 [43], Pfam [44], and SCOPE [45] databases using hhblits 3.1.0 and the following options: -Z 250 -z 1 -b 1 -B 250, minimum probability score of 95 [46,47]. Predicted protein sequences were also clustered de novo with a similar pipeline as previously used on virophages [12]. Briefly, predicted protein sequences were first compared to each other in an all-vs.-all BlastP [41] (v2.10.0+, default parameters). InfoMap [48]

(v0.18.25, *-two-level* option) was then used to obtain a first level of protein clustering ("Protein clusters"). These protein clusters were further compared to each other using *hhsearch* as follows: first, all members of a cluster were aligned with *muscle* v3.8.1551 [49] (default parameters), then a profile was built from this alignment using *hhmake* v3.1.0 [47] with the options *-M 50* and *-add\_cons*. Profiles were then compared all-vs-all with *hhsearch* v3.1.0 [47] with option *-norealign* and maximum E-value of 0.001. Hits between clusters displaying a probability score  $\geq 90$  and covering  $\geq 50\%$  of the shorter alignment, or a probability score  $\geq 99$  and covering  $\geq 20\%$  of the shorter alignment, were compiled and used as input for a greedy clustering to establish "superclusters," i.e., groups of related protein clusters.

Individual predicted functional protein annotations were then summarized at the protein cluster and supercluster levels by assigning the cluster/superclusters to the majority assignment among its members if it included more than 33% of its members. Superclusters corresponding to the canonical viroplasm morphogenesis gene module were identified based on an assignment to 3J26\_N (Penton), 3J26\_I (MCP), 4EKF\_A (PRO), or the Pfam Clan: P-loop\_NTPase (CL0023, ATPase). These 4 superclusters were further validated by verifying that all corresponding genes from reference viroplasm genomes belonged to the expected supercluster, and no other supercluster could be assigned to one of these four domains/clans. These four superclusters were further refined to remove clusters that correspond to partial and/or duplicated genes. This resulted in a final set of three clusters for MCP, one for PRO, two for ATPase, and 11 for Penton.

To obtain a final systematic detection of these core genes across all genomes and for external datasets, HMM profiles were built for these sequences as follows. For each supercluster, protein sequences were compared to each other in an all-vs-all BlastP [41] (v2.10.0+, default parameters), clustered using MCL 14-137 (inflation parameter = 5) [50], and a multiple alignments and HMM profile were built using MAFFT v7.490 [51] and *hmmbuild* v3.3.2 [37], respectively, for each group of ten sequences or more. This process yielded 19 HMM profiles (7 MCP, 2 PRO, 4 ATPase, 7 Penton), which were used to identify the four morphogenesis genes in each of the 848 non-redundant viroplasm genomes (*hmmsearch* v3.3.2 [37], minimum score of 50, best hit by genome). The sequence divergence for each of the four morphogenesis genes was then evaluated by calculating all-vs-all pairwise amino-acid identity percentage with SDT [52] (Feb 2014 version, default parameters).

#### 4.5. Rooted Phylogenetic Trees for ATPase and PRO Genes

The ATPase and PRO genes have homologs in non-viroplasm genomes, which provides an opportunity to verify that viroplasm form a monophyletic clade with respect to these other sequences. To that end, two categories of outgroup sequences were included: (i) sequences previously used in similar analyses [20], and (ii) NCBI nr sequences not affiliated to viroplasm (*Lavidaviridae*) but similar to a viroplasm (BLAST score  $\geq 100$ ). For each marker (ATPase and PRO), the resulting viroplasm and outgroup sequences were clustered using MCL 14-137 (inflation parameter = 4 for PRO and 9 for ATPase) [50], and one representative of each cluster was selected, prioritizing isolate over metagenome-derived genomes.

For each set of representatives, multiple alignments were computed with MAFFT v7.490 [51] (*-auto* option). The alignment was visually inspected to remove partial and non-homologous sequences (i.e., lacking conserved regions or residues). IQ-Tree v1.5.5 [53] was then used to build a tree for each curated alignment, with automatic detection of the most appropriate substitution matrix and 1000 replicates of ultra-fast bootstraps. The best-fit model was LG+F+R7 for both PRO and ATPase.

#### 4.6. Identification and Analysis of Complete and Near-Complete Viroplasm Genomes

Among the 848 non-redundant viroplasm genomes, several categories of sequences were considered as likely representing complete and near-complete genomes: (i) reference genomes from isolates (n = 4), (ii) sequences identified as integrated with upstream and downstream host regions  $\geq 2$  kb (n = 7), (iii) sequences with direct or inverted terminal

repeats ( $n = 118$  and  $n = 8$ , respectively), (iv) sequences predicted to be  $\geq 90\%$  complete based on CheckV (AAI-based prediction,  $n = 59$ ), and (v) linear contigs  $\geq 25$  kb ( $n = 61$ ). This latter category was based on the median length of predicted complete and near-complete genomes from all other categories (25,168 bp). Overall, 257 sequences were considered complete or near-complete virophage genomes.

These complete and near-complete genomes were used as input for phylogenetic trees and genome-wide clustering to establish groups and potential taxa within the virophages. For phylogenetic trees, the sequences of the four morphogenesis genes detected in the 257 complete and near-complete genomes using the new HMM profiles (see above) were used after excluding all sequences that covered  $< 60\%$  of the HMM profile to remove partial gene predictions. Multiple alignments were then built for each gene using an iterative clustering-alignment-phylogeny procedure specifically adapted for aligning highly diverging sequences [54]. The alignments were then automatically trimmed using clipkit v1.3.0 [55] using the kpi-smart-gap mode to remove uninformative positions, and the trimmed alignments were used as input for tree building with IQ-Tree v2.2.0.3 [56] with automatic detection of the most appropriate substitution matrix, and 1000 replicates of ultra-fast bootstraps. The best-fit model was Q.pfam+F+R7 for PRO, Q.yeast+F+R8 for ATPase, and Q.pfam+F+R8 for both MCP and penton. For the larger MCP phylogeny, including both complete and partial virophage genomes (Figure S6), multiple alignments were computed with MAFFT v7.490 based on the curated multiple alignment including MCP from complete and near-complete genomes only (options “-add” and “-keeplength”) [51], and the phylogeny was built with tree IQ-Tree v2.2.0.3 [56] with similar parameters as described above.

Genome-wide amino acid identity (AAI) clustering was performed as in [57]. Briefly, predicted protein sequences from the 257 complete and near-complete virophages were compared all-vs-all using diamond v0.9.24.125 [58] and the following options: “-evaluate 1e-5 -max-target-seqs 10,000 -query-cover 50 -subject-cover 50”. The resulting file was used as input for the script “amino\_acid\_identity.py” to calculate the average AAI for all pairs of genomes. The script “filter\_aai.py” was then used to select only pairs of genomes with a minimum normalized cumulative bit score of 0.05. Finally, these selected pairwise AAI values were used as input for an MCL clustering using MCL 14-137 (inflation parameter = 1.1) [50].

#### 4.7. Identification of New Virophage Taxa, Delineation Criteria, and Classification Approach

To enable the identification and classification of new virophage genomes, an HMM and a BLAST database were prepared alongside adjusted cutoffs for each model and/or clade ([https://github.com/simroux/ICTV\\_VirophageSG](https://github.com/simroux/ICTV_VirophageSG), accessed on 15 November 2022). First, predicted proteins from the sequence to classify are searched for the virophage morphogenesis genes using hmmsearch and the new HMM profiles (see above “Genome annotation and de novo protein clustering”). A minimum score of 50 on at least one of the MCP profiles is required to automatically classify the input sequence in the *Maveriviricetes* class. A minimum score of 40 is used for the detection of the three other virophage genes (ATPase, PRO, Penton). Next, the MCP sequences are compared to MCPs from complete and near-complete genomes robustly classified in one of the seven new groups based on the combined phylogeny and genome clustering approaches using BlastP. New sequences are affiliated with one of the seven new groups based on the best BLAST hit, with the minimum bit score cutoff determined based on the highest score obtained for sequences outside the group (Table S2). Finally, a previously published PLV-associated HMM profile [12] was also searched using the same hmmsearch approach and a minimum score cutoff of 50 to identify PLV-like sequences. This approach was applied to the virophage dataset studied here as well as two external datasets: “Gossenköllesee” and “Adintovirus” (see above).

#### 4.8. Visualization

Boxplots and bar charts were created using the ggplot2 v3.3.6 package [59] in R v4.2.1 [60], with data processed using the dplyr v1.0.10 [61] and tidyr v1.2.1 [62] packages. Annotated phylogenetic trees were generated with the packages ggtree v3.4.2 [63–66] and ggtreeExtra v1.6.1 [67]. Coloring was based on palettes from ggpubfigs [68]. Genome maps were drawn with EasyFig v2.2.3 [69] based on genome annotation from NCBI GenBank, except for PE\_004, which was newly annotated here.

**Supplementary Materials:** The following supporting information can be downloaded at: <https://www.mdpi.com/article/10.3390/biom13020204/s1>, Figure S1: Length distribution of complete and near-complete virophage genomes; Figure S2: ATPase and Cysteine Protease (PRO) trees including virophage and outgroup sequences; Figure S3: Length distribution for the 4 virophage conserved morphogenesis genes; Figure S4: Characteristics of proposed virophage clades; Figure S5: Distribution of curated virophage groups on phylogenies built from other virophage markers; Figure S6: Virophage phylogeny (MCP) including complete, near-complete, and partial genomes; Figure S7: Gene content and genome maps of 5 Adintoviruses classified in the *Maveriviricetes* class and closest reference; Table S1: List and characteristics of the virophage sequences analyzed in this study, a number of metagenomes and/or virophage sequences included here were previously analyzed in [2,4–6,11–18,23,24,27–30,32,33,70–135]; Table S2: Cutoffs used for BLAST-based assignment to families within the *Maveriviricetes* class; Table S3: Result of marker-gene detection and BLAST-based affiliation on external datasets; Table S4: Characteristics of protist genomes in which virophages were detected, integrated virophage genomes in Cafeteria burkhardae were identified in a previous study [28].

**Author Contributions:** Conceptualization, S.R., M.G.F., F.S. and N.Y.; methodology, S.R., M.G.F., F.S. and N.Y.; software, S.R.; formal analysis, S.R., M.G.F., T.H., L.A.K., F.S. and N.Y.; writing—original draft preparation, S.R., M.G.F., F.S. and N.Y.; writing—review and editing, S.R., M.G.F., T.H., L.A.K., F.S. and N.Y. All authors have read and agreed to the published version of the manuscript.

**Funding:** The work conducted by the U.S. Department of Energy Joint Genome Institute (<https://ror.org/04xm1d337>), a DOE Office of Science User Facility, is supported by the Office of Science of the U.S. Department of Energy operated under Contract No. DE-AC02-05CH11231. M.G.F. acknowledges funding from the Max Planck Society. L.A.K. is supported by NIH grant R15HG010409 and NSF grant DEB-1651908.

**Institutional Review Board Statement:** Not applicable.

**Informed Consent Statement:** Not applicable.

**Data Availability Statement:** The list of all virophage genomes used in this study is provided in Table S1, along with the associated publications and JGI proposal DOIs, when available. The corresponding sequences, along with the reference MCP alignment and phylogeny, are provided at <https://portal.nersc.gov/cfs/m342/virophages/> (accessed on 5 January 2023). The database and script used for the virophage sequence assignment are provided at [https://github.com/simroux/ICTV\\_VirophageSG](https://github.com/simroux/ICTV_VirophageSG) (accessed on 5 January 2023).

**Acknowledgments:** The authors would like to thank Stephen Nayfach for helpful discussions about comparative genomic analysis.

**Conflicts of Interest:** The authors declare no conflict of interest.

## References

1. Claverie, J.-M.; Abergel, C. Mimivirus and Its Virophage. *Annu. Rev. Genet.* **2009**, *43*, 49–66. [[CrossRef](#)] [[PubMed](#)]
2. Mougari, S.; Sahmi-Bounsiar, D.; Levasseur, A.; Colson, P.; La Scola, B. Virophages of Giant Viruses: An Update at Eleven. *Viruses* **2019**, *11*, 733. [[CrossRef](#)] [[PubMed](#)]
3. Duponchel, S.; Fischer, M.G. Viva Lavidaviruses! Five Features of Virophages That Parasitize Giant DNA Viruses. *PLOS Pathog.* **2019**, *15*, e1007592. [[CrossRef](#)] [[PubMed](#)]
4. La Scola, B.; Desnues, C.; Pagnier, I.; Robert, C.; Barrassi, L.; Fournous, G.; Suzan-Monti, M.; Forterre, P.; Koonin, E.; Raoult, D.; et al. The Virophage as a Unique Parasite of the Giant Mimivirus. *Nature* **2008**, *455*, 100–104. [[CrossRef](#)]
5. Fischer, M.G.; Suttle, C.A. A Virophage at the Origin of Large DNA Transposons. *Science* **2011**, *332*, 231–234. [[CrossRef](#)]

6. Sheng, Y.; Wu, Z.; Xu, S.; Wang, Y. Isolation and Identification of a Large Green Alga Virus (Chlorella Virus XW01) of Mimiviridae and Its Virophage (Chlorella Virus Virophage SW01) by Using Unicellular Green Algal Cultures. *J. Virol.* **2022**, *96*, e02114–21. [[CrossRef](#)]
7. Gaia, M.; Benamar, S.; Boughalmi, M.; Pagnier, I.; Croce, O.; Colson, P.; Raoult, D.; Scola, B.L. Zamilon, a Novel Virophage with Mimiviridae Host Specificity. *PLoS ONE* **2014**, *9*, e94923. [[CrossRef](#)]
8. Fischer, M.G. The Virophage Family Lavidaviridae. *Curr. Issues Mol. Biol.* **2021**, *40*, 1–24. [[CrossRef](#)]
9. Krupovic, M.; Kuhn, J.H.; Fischer, M.G. A Classification System for Virophages and Satellite Viruses. *Arch. Virol.* **2016**, *161*, 233–247. [[CrossRef](#)]
10. Gorbalenya, A.E.; Krupovic, M.; Mushegian, A.; Kropinski, A.M.; Siddell, S.G.; Varsani, A.; Adams, M.J.; Davison, A.J.; Dutilh, B.E.; Harrach, B.; et al. The New Scope of Virus Taxonomy: Partitioning the Virosphere into 15 Hierarchical Ranks. *Nat. Microbiol.* **2020**, *5*, 668–674. [[CrossRef](#)]
11. Yutin, N.; Kapitonov, V.V.; Koonin, E.V. A New Family of Hybrid Virophages from an Animal Gut Metagenome. *Biol. Direct* **2015**, *10*, 19. [[CrossRef](#)] [[PubMed](#)]
12. Páez-Espino, D.; Zhou, J.; Roux, S.; Nayfach, S.; Pavlopoulos, G.A.; Schulz, F.; McMahon, K.D.; Walsh, D.; Woyke, T.; Ivanova, N.N.; et al. Diversity, Evolution, and Classification of Virophages Uncovered through Global Metagenomics. *Microbiome* **2019**, *7*, 157. [[CrossRef](#)] [[PubMed](#)]
13. Yau, S.; Lauro, F.M.; DeMaere, M.Z.; Brown, M.V.; Thomas, T.; Raftery, M.J.; Andrews-Pfannkoch, C.; Lewis, M.; Hoffman, J.M.; Gibson, J.A.; et al. Virophage Control of Antarctic Algal Host-Virus Dynamics. *Proc. Natl. Acad. Sci. USA* **2011**, *108*, 6163–6168. [[CrossRef](#)]
14. Zhou, J.; Zhang, W.; Yan, S.; Xiao, J.; Zhang, Y.; Li, B.; Pan, Y.; Wang, Y. Diversity of Virophages in Metagenomic Data Sets. *J. Virol.* **2013**, *87*, 4225–4236. [[CrossRef](#)] [[PubMed](#)]
15. Zhou, J.; Sun, D.; Childers, A.; McDermott, T.R.; Wang, Y.; Liles, M.R. Three Novel Virophage Genomes Discovered from Yellowstone Lake Metagenomes. *J. Virol.* **2015**, *89*, 1278–1285. [[CrossRef](#)]
16. Roux, S.; Chan, L.K.; Egan, R.; Malmstrom, R.R.; McMahon, K.D.; Sullivan, M.B. Ecogenomics of Virophages and Their Giant Virus Hosts Assessed through Time Series Metagenomics. *Nat. Commun.* **2017**, *8*, 858. [[CrossRef](#)]
17. Gong, C.; Zhang, W.; Zhou, X.; Wang, H.; Sun, G.; Xiao, J.; Pan, Y.; Yan, S.; Wang, Y. Novel Virophages Discovered in a Freshwater Lake in China. *Front. Microbiol.* **2016**, *7*, 5. [[CrossRef](#)]
18. Oh, S.; Yoo, D.; Liu, W.-T.T. Metagenomics Reveals a Novel Virophage Population in a Tibetan Mountain Lake. *Microbes Environ.* **2016**, *31*, 173–177. [[CrossRef](#)]
19. Bellas, C.M.; Sommaruga, R. Polinton-like Viruses Are Abundant in Aquatic Ecosystems. *Microbiome* **2021**, *9*, 13. [[CrossRef](#)]
20. Yutin, N.; Raoult, D.; Koonin, E.V. Virophages, Polintons, and Transpovirons: A Complex Evolutionary Network of Diverse Selfish Genetic Elements with Different Reproduction Strategies. *Virol. J.* **2013**, *10*, 158. [[CrossRef](#)]
21. Yutin, N.; Shevchenko, S.; Kapitonov, V.; Krupovic, M.; Koonin, E.V. A Novel Group of Diverse Polinton-like Viruses Discovered by Metagenome Analysis. *BMC Biol.* **2015**, *13*, 95. [[CrossRef](#)] [[PubMed](#)]
22. Krupovic, M.; Koonin, E.V. Polintons: A Hotbed of Eukaryotic Virus, Transposon and Plasmid Evolution. *Nat. Rev. Microbiol.* **2015**, *13*, 105–115. [[CrossRef](#)] [[PubMed](#)]
23. Starrett, G.J.; Tisza, M.J.; Welch, N.L.; Belford, A.K.; Peretti, A.; Pastrana, D.V.; Buck, C.B. Adintoviruses: A Proposed Animal-Tropic Family of Midsize Eukaryotic Linear DsDNA (MELD) Viruses. *Virus Evol.* **2021**, *7*, veaa055. [[CrossRef](#)] [[PubMed](#)]
24. Santini, S.; Jeudy, S.; Bartoli, J.; Poirot, O.; Lescot, M.; Abergel, C.; Barbe, V. Genome of Phaeocystis Globosa Virus PgV-16T Highlights the Common Ancestry of the Largest Known DNA Viruses Infecting Eukaryotes. *Proc. Natl. Acad. Sci. USA* **2013**, *110*, 10800–10805. [[CrossRef](#)] [[PubMed](#)]
25. Roitman, S.; Rozenberg, A.; Lavy, T.; Brussaard, C.P.D.; Kleifeld, O.; Béjà, O. Infection Cycle and Phylogeny of the Polinton-like Virus Phaeocystis Globosa Virus Virophage-14T. *bioRxiv* **2022**. [[CrossRef](#)]
26. Krupovic, M.; Bamford, D.H.; Koonin, E.V. Conservation of Major and Minor Jelly-Roll Capsid Proteins in Polinton (Maverick) Transposons Suggests That They Are Bona Fide Viruses. *Biol. Direct* **2014**, *9*, 6. [[CrossRef](#)]
27. Fischer, M.G.; Hackl, T. Host Genome Integration and Giant Virus-Induced Reactivation of the Virophage Mavirus. *Nature* **2016**, *540*, 288–291. [[CrossRef](#)]
28. Hackl, T.; Duponchel, S.; Barenhoff, K.; Weinmann, A.; Fischer, M.G. Virophages and Retrotransposons Colonize the Genomes of a Heterotrophic Flagellate. *eLife* **2021**, *10*, e72674. [[CrossRef](#)]
29. Stough, J.M.A.; Yutin, N.; Chaban, Y.V.; Moniruzzaman, M.; Gann, E.R.; Pound, H.L.; Steffen, M.M.; Black, J.N.; Koonin, E.V.; Wilhelm, S.W.; et al. Genome and Environmental Activity of a Chrysochromulina Parva Virus and Its Virophages. *Front. Microbiol.* **2019**, *10*, 703. [[CrossRef](#)]
30. Roux, S.; Páez-Espino, D.; Chen, I.-M.A.; Palaniappan, K.; Ratner, A.; Chu, K.; Reddy, T.B.K.; Nayfach, S.; Schulz, F.; Call, L.; et al. IMG/VR v3: An Integrated Ecological and Evolutionary Framework for Interrogating Genomes of Uncultivated Viruses. *Nucleic Acids Res.* **2020**, *49*, D764–D775. [[CrossRef](#)]
31. Roux, S.; Adriaenssens, E.M.; Dutilh, B.E.; Koonin, E.V.; Kropinski, A.M.; Krupovic, M.; Kuhn, J.H.; Lavigne, R.; Brister, J.R.; Varsani, A.; et al. Minimum Information about an Uncultivated Virus Genome (MIUVIG). *Nat. Biotechnol.* **2019**, *37*, 29–37. [[CrossRef](#)] [[PubMed](#)]



32. Tisza, M.J.; Buck, C.B. A Catalog of Tens of Thousands of Viruses from Human Metagenomes Reveals Hidden Associations with Chronic Diseases. *Proc. Natl. Acad. Sci. USA* **2021**, *118*, e2023202118. [[CrossRef](#)] [[PubMed](#)]
33. Wallace, M.A.; Coffman, K.A.; Gilbert, C.; Ravindran, S.; Albery, G.F.; Abbott, J.; Argyridou, E.; Bellosta, P.; Betancourt, A.J.; Colinet, H.; et al. The Discovery, Distribution, and Diversity of DNA Viruses Associated with *Drosophila Melanogaster* in Europe. *Virus Evol.* **2021**, *7*, veab031. [[CrossRef](#)] [[PubMed](#)]
34. Castillo, Y.M.; Forn, I.; Yau, S.; Morán, X.A.G.; Alonso-Sáez, L.; Arandia-Gorostidi, N.; Vaqué, D.; Sebastián, M. Seasonal Dynamics of Natural *Ostreococcus* Viral Infection at the Single Cell Level Using VirusFISH. *Environ. Microbiol.* **2021**, *23*, 3009–3019. [[CrossRef](#)]
35. del Arco, A.; Fischer, M.; Becks, L. Simultaneous Giant Virus and Virophage Quantification Using Droplet Digital PCR. *Viruses* **2022**, *14*, 1056. [[CrossRef](#)]
36. Levasseur, A.; Bekliz, M.; Chabrière, E.; Pontarotti, P.; Scola, B.L.; Raoult, D. MIMIVIRE Is a Defence System in Mimivirus That Confers Resistance to Virophage. *Nature* **2016**, *531*, 249–252. [[CrossRef](#)]
37. Eddy, S.R. Accelerated Profile HMM Searches. *PLoS Comput. Biol.* **2011**, *7*, e1002195. [[CrossRef](#)]
38. Mukherjee, S.; Stamatis, D.; Bertsch, J.; Ovchinnikova, G.; Sundaramurthi, J.C.; Lee, J.; Kandimalla, M.; Chen, I.-M.A.; Kyrpides, N.C.; Reddy, T.B.K. Genomes OnLine Database (GOLD) v.8: Overview and Updates. *Nucleic Acids Res.* **2021**, *49*, D723–D733. [[CrossRef](#)]
39. O’Leary, N.A.; Wright, M.W.; Brister, J.R.; Ciufu, S.; Haddad, D.; McVeigh, R.; Rajput, B.; Robbertse, B.; Smith-White, B.; Ako-Adjei, D.; et al. Reference Sequence (RefSeq) Database at NCBI: Current Status, Taxonomic Expansion, and Functional Annotation. *Nucleic Acids Res.* **2016**, *44*, D733–D745. [[CrossRef](#)]
40. Delcher, A.L.; Salzberg, S.L.; Phillippy, A.M. Using MUMmer to Identify Similar Regions in Large Sequence Sets. *Curr. Protoc. Bioinform.* **2003**, *10*, 10.3. [[CrossRef](#)]
41. Camacho, C.; Coulouris, G.; Avagyan, V.; Ma, N.; Papadopoulos, J.; Bealer, K.; Madden, T.L. BLAST+: Architecture and Applications. *BMC Bioinform.* **2009**, *10*, 421. [[CrossRef](#)] [[PubMed](#)]
42. Hyatt, D.; Chen, G.-L.; LoCascio, P.F.; Land, M.L.; Larimer, F.W.; Hauser, L.J. Prodigal: Prokaryotic Gene Recognition and Translation Initiation Site Identification. *BMC Bioinform.* **2010**, *11*, 119. [[CrossRef](#)] [[PubMed](#)]
43. Berman, H.; Henrick, K.; Nakamura, H. Announcing the Worldwide Protein Data Bank. *Nat. Struct. Mol. Biol.* **2003**, *10*, 980. [[CrossRef](#)] [[PubMed](#)]
44. El-Gebali, S.; Mistry, J.; Bateman, A.; Eddy, S.R.; Luciani, A.; Potter, S.C.; Qureshi, M.; Richardson, L.J.; Salazar, G.A.; Smart, A.; et al. The Pfam Protein Families Database in 2019. *Nucleic Acids Res.* **2019**, *47*, D427–D432. [[CrossRef](#)]
45. Chandonia, J.-M.; Fox, N.K.; Brenner, S.E. SCOPe: Manual Curation and Artifact Removal in the Structural Classification of Proteins – Extended Database. *J. Mol. Biol.* **2017**, *429*, 348–355. [[CrossRef](#)] [[PubMed](#)]
46. Remmert, M.; Biegert, A.; Hauser, A.; Söding, J. HHblits: Lightning-Fast Iterative Protein Sequence Searching by HMM-HMM Alignment. *Nat. Methods* **2012**, *9*, 173–175. [[CrossRef](#)]
47. Steinegger, M.; Meier, M.; Mirdita, M.; Vöhringer, H.; Haunsberger, S.J.; Söding, J. HH-Suite3 for Fast Remote Homology Detection and Deep Protein Annotation. *BMC Bioinform.* **2019**, *20*, 473. [[CrossRef](#)]
48. Edler, D.; Bohlin, L.; Rosvall, M. Mapping Higher-Order Network Flows in Memory and Multilayer Networks with Infomap. *Algorithms* **2017**, *10*, 112. [[CrossRef](#)]
49. Edgar, R.C. MUSCLE: A Multiple Sequence Alignment Method with Reduced Time and Space Complexity. *BMC Bioinform.* **2004**, *5*, 113. [[CrossRef](#)]
50. van Dongen, S.; Abreu-Goodger, C. Using MCL to Extract Clusters from Networks. In *Bacterial Molecular Networks: Methods and Protocols*; van Helden, J., Toussaint, A., Thieffry, D., Eds.; Methods in Molecular Biology; Springer: New York, NY, USA, 2012; pp. 281–295. ISBN 978-1-61779-361-5.
51. Katoh, K.; Standley, D.M. MAFFT Multiple Sequence Alignment Software Version 7: Improvements in Performance and Usability. *Mol. Biol. Evol.* **2013**, *30*, 772–780. [[CrossRef](#)]
52. Muhire, B.M.; Varsani, A.; Martin, D.P. SDT: A Virus Classification Tool Based on Pairwise Sequence Alignment and Identity Calculation. *PLoS ONE* **2014**, *9*, e108277. [[CrossRef](#)]
53. Nguyen, L.-T.; Schmidt, H.A.; von Haeseler, A.; Minh, B.Q. IQ-TREE: A Fast and Effective Stochastic Algorithm for Estimating Maximum-Likelihood Phylogenies. *Mol. Biol. Evol.* **2015**, *32*, 268–274. [[CrossRef](#)] [[PubMed](#)]
54. Wolf, Y.I.; Kazlauskas, D.; Iranzo, J.; Lucía-Sanz, A.; Kuhn, J.H.; Krupovic, M.; Dolja, V.V.; Koonin, E.V. Origins and Evolution of the Global RNA Virome. *mBio* **2018**, *9*, e02329-18. [[CrossRef](#)] [[PubMed](#)]
55. Steenwyk, J.L.; Iii, T.J.B.; Li, Y.; Shen, X.-X.; Rokas, A. ClipKIT: A Multiple Sequence Alignment Trimming Software for Accurate Phylogenomic Inference. *PLoS Biol.* **2020**, *18*, e3001007. [[CrossRef](#)] [[PubMed](#)]
56. Minh, B.Q.; Schmidt, H.A.; Chernomor, O.; Schrempf, D.; Woodhams, M.D.; von Haeseler, A.; Lanfear, R. IQ-TREE 2: New Models and Efficient Methods for Phylogenetic Inference in the Genomic Era. *Mol. Biol. Evol.* **2020**, *37*, 1530–1534. [[CrossRef](#)] [[PubMed](#)]
57. Nayfach, S.; Páez-Espino, D.; Call, L.; Low, S.J.; Sberro, H.; Ivanova, N.N.; Proal, A.D.; Fischbach, M.A.; Bhatt, A.S.; Hugenholtz, P.; et al. Metagenomic Compendium of 189,680 DNA Viruses from the Human Gut Microbiome. *Nat. Microbiol.* **2021**, *6*, 960–970. [[CrossRef](#)] [[PubMed](#)]
58. Buchfink, B.; Xie, C.; Huson, D.H. Fast and Sensitive Protein Alignment Using DIAMOND. *Nat. Methods* **2015**, *12*, 59–60. [[CrossRef](#)] [[PubMed](#)]

59. Wickham, H. *Ggplot2: Elegant Graphics for Data Analysis*; Springer: New York, NY, USA, 2016; ISBN 978-3-319-24277-4.
60. R Core Team. *R: A Language and Environment for Statistical Computing*; R Foundation for Statistical Computing: Vienna, Austria, 2022.
61. Wickham, H.; François, R.; Henry, L.; Müller, K. *Dplyr: A Grammar of Data Manipulation*, 2022.
62. Wickham, H.; Girlich, M. *Tidyr: Tidy Messy Data*, 2022.
63. Yu, G. Using Ggtree to Visualize Data on Tree-Like Structures. *Curr. Protoc. Bioinform.* **2020**, *69*, e96. [[CrossRef](#)]
64. Yu, G.; Lam, T.T.-Y.; Zhu, H.; Guan, Y. Two Methods for Mapping and Visualizing Associated Data on Phylogeny Using Ggtree. *Mol. Biol. Evol.* **2018**, *35*, 3041–3043. [[CrossRef](#)]
65. Yu, G.; Smith, D.; Zhu, H.; Guan, Y.; Lam, T.T.-Y. Ggtree: An R Package for Visualization and Annotation of Phylogenetic Trees with Their Covariates and Other Associated Data. *Methods Ecol. Evol.* **2017**, *8*, 28–36. [[CrossRef](#)]
66. Yu, G. *Data Integration, Manipulation and Visualization of Phylogenetic Trees*, 1st ed.; Chapman and Hall/CRC: Boca Raton, FL, USA, 2022. [[CrossRef](#)]
67. Xu, S.; Dai, Z.; Guo, P.; Fu, X.; Liu, S.; Zhou, L.; Tang, W.; Feng, T.; Chen, M.; Zhan, L.; et al. GgtreeExtra: Compact Visualization of Richly Annotated Phylogenetic Data. *Mol. Biol. Evol.* **2021**, *38*, 4039–4042. [[CrossRef](#)] [[PubMed](#)]
68. Steenwyk, J.L.; Rokas, A. Ggpubfigs: Colorblind-Friendly Color Palettes and Ggplot2 Graphic System Extensions for Publication-Quality Scientific Figures. *Microbiol. Resour. Announc.* **2021**, *10*, e00871-21. [[CrossRef](#)] [[PubMed](#)]
69. Sullivan, M.J.; Petty, N.K.; Beatson, S.A. Easyfig: A Genome Comparison Visualizer. *Bioinformatics* **2011**, *27*, 1009–1010. [[CrossRef](#)]
70. Lavy, A.; McGrath, D.G.; Matheus Carnevali, P.B.; Wan, J.; Dong, W.; Tokunaga, T.K.; Thomas, B.C.; Williams, K.H.; Hubbard, S.S.; Banfield, J.F. Microbial Communities across a Hillslope-riparian Transect Shaped by Proximity to the Stream, Groundwater Table, and Weathered Bedrock. *Ecol. Evol.* **2019**, *9*, 6869–6900. [[CrossRef](#)] [[PubMed](#)]
71. Linz, A.M.; Aylward, F.O.; Bertilsson, S.; McMahon, K.D. Time-series Metatranscriptomes Reveal Conserved Patterns between Phototrophic and Heterotrophic Microbes in Diverse Freshwater Systems. *Limnol. Oceanogr.* **2020**, *65*, S101–S112. [[CrossRef](#)]
72. Waldo, N.B.; Chistoserdova, L.; Hu, D.; Gough, H.L.; Neumann, R.B. Impacts of The Wetland Sedge *Carex Aquatilis* on Microbial Community and Methane Metabolisms. *Plant Soil* **2022**, *471*, 491–506. [[CrossRef](#)]
73. Borges, I.A.; de Assis, F.L.; Silva, L.K.; dos Santos Silva, L.K.; Abrahão, J. Rio Negro Virophage: Sequencing of the near Complete Genome and Transmission Electron Microscopy of Viral Factories and Particles. *Braz. J. Microbiol.* **2018**, *49*, 260–261. [[CrossRef](#)]
74. Rozmarynowycz, M.J.; Beall, B.F.N.; Bullerjahn, G.S.; Small, G.E.; Sterner, R.W.; Brovold, S.S.; D'souza, N.A.; Watson, S.B.; McKay, R.M.L. Transitions in Microbial Communities along a 1600 Km Freshwater Trophic Gradient. *J. Great Lakes Res.* **2019**, *45*, 263–276. [[CrossRef](#)]
75. Kelly, C.N.; Schwaner, G.W.; Cumming, J.R.; Driscoll, T.P. Metagenomic Reconstruction of Nitrogen and Carbon Cycling Pathways in Forest Soil: Influence of Different Hardwood Tree Species. *Soil Biol. Biochem.* **2021**, *156*, 108226. [[CrossRef](#)]
76. Wang, Y.; Zhao, R.; Liu, L.; Li, B.; Zhang, T. Selective Enrichment of Comammox from Activated Sludge Using Antibiotics. *Water Res.* **2021**, *197*, 117087. [[CrossRef](#)]
77. Kantor, R.S.; Huddy, R.J.; Iyer, R.; Thomas, B.C.; Brown, C.T.; Anantharaman, K.; Tringe, S.; Hettich, R.L.; Harrison, S.T.L.; Banfield, J.F. Genome-Resolved Meta-Omics Ties Microbial Dynamics to Process Performance in Biotechnology for Thiocyanate Degradation. *Environ. Sci. Technol.* **2017**, *51*, 2944–2953. [[CrossRef](#)] [[PubMed](#)]
78. An, D.; Caffrey, S.M.; Soh, J.; Agrawal, A.; Brown, D.; Budwill, K.; Dong, X.; Dunfield, P.F.; Foght, J.; Gieg, L.M.; et al. Metagenomics of Hydrocarbon Resource Environments Indicates Aerobic Taxa and Genes to Be Unexpectedly Common. *Environ. Sci. Technol.* **2013**, *47*, 10708–10717. [[CrossRef](#)] [[PubMed](#)]
79. Sabuda, M.C.; Putman, L.L.; Hoehler, T.M.; Kubo, M.D.; Brazelton, W.J.; Cardace, D.; Schrenk, M.O. Biogeochemical Gradients in a Serpentinization-Influenced Aquifer: Implications for Gas Exchange Between the Subsurface and Atmosphere. *J. Geophys. Res. Biogeosci.* **2021**, *126*, e2020JG006209. [[CrossRef](#)]
80. Bendall, M.L.; Stevens, S.L.; Chan, L.-K.; Malfatti, S.; Schwientek, P.; Tremblay, J.; Schackwitz, W.; Martin, J.; Pati, A.; Bushnell, B.; et al. Genome-Wide Selective Sweeps and Gene-Specific Sweeps in Natural Bacterial Populations. *ISME J.* **2016**, *10*, 1589–1601. [[CrossRef](#)]
81. Spang, A.; Saw, J.H.; Jørgensen, S.L.; Zaremba-Niedzwiedzka, K.; Martijn, J.; Lind, A.E.; van Eijk, R.; Schleper, C.; Guy, L.; Ettema, T.J.G. Complex Archaea That Bridge the Gap between Prokaryotes and Eukaryotes. *Nature* **2015**, *521*, 173–179. [[CrossRef](#)]
82. Roux, S.; Brum, J.R.; Dutilh, B.E.; Sunagawa, S.; Duhaime, M.B.; Loy, A.; Poulos, B.T.; Solonenko, N.; Lara, E.; Poulain, J.; et al. Ecogenomics and Potential Biogeochemical Impacts of Uncultivated Globally Abundant Ocean Viruses. *Nature* **2016**, *537*, 689–693. [[CrossRef](#)]
83. MetaHIT Consortium; Nielsen, H.B.; Almeida, M.; Juncker, A.S.; Rasmussen, S.; Li, J.; Sunagawa, S.; Plichta, D.R.; Gautier, L.; Pedersen, A.G.; et al. Identification and Assembly of Genomes and Genetic Elements in Complex Metagenomic Samples without Using Reference Genomes. *Nat. Biotechnol.* **2014**, *32*, 822–828. [[CrossRef](#)]
84. Levy-Booth, D.J.; Giesbrecht, I.J.W.; Kellogg, C.T.E.; Heger, T.J.; D'Amore, D.V.; Keeling, P.J.; Hallam, S.J.; Mohn, W.W. Seasonal and Ecohydrological Regulation of Active Microbial Populations Involved in DOC, CO<sub>2</sub>, and CH<sub>4</sub> Fluxes in Temperate Rainforest Soil. *ISME J.* **2019**, *13*, 950–963. [[CrossRef](#)]
85. Krüger, K.; Chafee, M.; Ben Francis, T.; Glavina del Rio, T.; Becher, D.; Schweder, T.; Amann, R.I.; Teeling, H. In Marine Bacteroidetes the Bulk of Glycan Degradation during Algae Blooms Is Mediated by Few Clades Using a Restricted Set of Genes. *ISME J.* **2019**, *13*, 2800–2816. [[CrossRef](#)]

86. Jeudy, S.; Bertaux, L.; Alempic, J.-M.; Lartigue, A.; Legendre, M.; Belmudes, L.; Santini, S.; Philippe, N.; Beucher, L.; Biondi, E.G.; et al. Exploration of the Propagation of Transpovirons within Mimiviridae Reveals a Unique Example of Commensalism in the Viral World. *ISME J.* **2020**, *14*, 727–739. [[CrossRef](#)]
87. St. James, A.R.; Yavitt, J.B.; Zinder, S.H.; Richardson, R.E. Linking Microbial Sphagnum Degradation and Acetate Mineralization in Acidic Peat Bogs: From Global Insights to a Genome-Centric Case Study. *ISME J.* **2021**, *15*, 293–303. [[CrossRef](#)] [[PubMed](#)]
88. Gazitúa, M.C.; Vik, D.R.; Roux, S.; Gregory, A.C.; Bolduc, B.; Widner, B.; Mulholland, M.R.; Hallam, S.J.; Ulloa, O.; Sullivan, M.B. Potential Virus-Mediated Nitrogen Cycling in Oxygen-Depleted Oceanic Waters. *ISME J.* **2021**, *15*, 981–998. [[CrossRef](#)] [[PubMed](#)]
89. Berg, M.; Goudeau, D.; Olmsted, C.; McMahan, K.D.; Yitbarek, S.; Thweatt, J.L.; Bryant, D.A.; Eloë-Fadrosh, E.A.; Malmstrom, R.R.; Roux, S. Host Population Diversity as a Driver of Viral Infection Cycle in Wild Populations of Green Sulfur Bacteria with Long Standing Virus-Host Interactions. *ISME J.* **2021**, *15*, 1569–1584. [[CrossRef](#)]
90. Tsuji, J.M.; Tran, N.; Schiff, S.L.; Venkiteswaran, J.J.; Molot, L.A.; Tank, M.; Hanada, S.; Neufeld, J.D. Anoxygenic Photosynthesis and Iron–Sulfur Metabolic Potential of Chlorobia Populations from Seasonally Anoxic Boreal Shield Lakes. *ISME J.* **2020**, *14*, 2732–2747. [[CrossRef](#)] [[PubMed](#)]
91. Tran, P.Q.; Bachand, S.C.; McIntyre, P.B.; Kraemer, B.M.; Vadeboncoeur, Y.; Kimirei, I.A.; Tamatamah, R.; McMahan, K.D.; Anantharaman, K. Depth-Discrete Metagenomics Reveals the Roles of Microbes in Biogeochemical Cycling in the Tropical Freshwater Lake Tanganyika. *ISME J.* **2021**, *15*, 1971–1986. [[CrossRef](#)] [[PubMed](#)]
92. Francis, T.B.; Bartosik, D.; Sura, T.; Sichert, A.; Hehemann, J.-H.; Markert, S.; Schweder, T.; Fuchs, B.M.; Teeling, H.; Amann, R.L.; et al. Changing Expression Patterns of TonB-Dependent Transporters Suggest Shifts in Polysaccharide Consumption over the Course of a Spring Phytoplankton Bloom. *ISME J.* **2021**, *15*, 2336–2350. [[CrossRef](#)]
93. Zhou, J.; Theroux, S.M.; Bueno de Mesquita, C.P.; Hartman, W.H.; Tian, Y.; Tringe, S.G. Microbial Drivers of Methane Emissions from Unrestored Industrial Salt Ponds. *ISME J.* **2022**, *16*, 284–295. [[CrossRef](#)]
94. Jurgensen, S.K.; Roux, S.; Schwenck, S.M.; Stewart, F.J.; Sullivan, M.B.; Brum, J.R. Viral Community Analysis in a Marine Oxygen Minimum Zone Indicates Increased Potential for Viral Manipulation of Microbial Physiological State. *ISME J.* **2022**, *16*, 972–982. [[CrossRef](#)]
95. Angle, J.C.; Morin, T.H.; Solden, L.M.; Narrowe, A.B.; Smith, G.J.; Borton, M.A.; Rey-Sanchez, C.; Daly, R.A.; Mirfenderesgi, G.; Hoyt, D.W.; et al. Methanogenesis in Oxygenated Soils Is a Substantial Fraction of Wetland Methane Emissions. *Nat. Commun.* **2017**, *8*, 1567. [[CrossRef](#)]
96. Dombrowski, N.; Teske, A.P.; Baker, B.J. Expansive Microbial Metabolic Versatility and Biodiversity in Dynamic Guaymas Basin Hydrothermal Sediments. *Nat. Commun.* **2018**, *9*, 4999. [[CrossRef](#)]
97. Sorensen, J.W.; Dunivin, T.K.; Tobin, T.C.; Shade, A. Ecological Selection for Small Microbial Genomes along a Temperate-to-Thermal Soil Gradient. *Nat. Microbiol.* **2019**, *4*, 55–61. [[CrossRef](#)] [[PubMed](#)]
98. Daly, R.A.; Roux, S.; Borton, M.A.; Morgan, D.M.; Johnston, M.D.; Booker, A.E.; Hoyt, D.W.; Meulia, T.; Wolfe, R.A.; Hanson, A.J.; et al. Viruses Control Dominant Bacteria Colonizing the Terrestrial Deep Biosphere after Hydraulic Fracturing. *Nat. Microbiol.* **2019**, *4*, 352–361. [[CrossRef](#)]
99. Woodcroft, B.J.; Singleton, C.M.; Boyd, J.A.; Evans, P.N.; Emerson, J.B.; Zayed, A.A.F.; Hoelzle, R.D.; Lamberton, T.O.; McCalley, C.K.; Hodgkins, S.B.; et al. Genome-Centric View of Carbon Processing in Thawing Permafrost. *Nature* **2018**, *560*, 49–54. [[CrossRef](#)]
100. Nayfach, S.; Camargo, A.P.; Schulz, F.; Eloë-Fadrosh, E.; Roux, S.; Kyrpides, N.C. CheckV Assesses the Quality and Completeness of Metagenome-Assembled Viral Genomes. *Nat. Biotechnol.* **2020**, *39*, 578–585. [[CrossRef](#)]
101. Hackl, T.; Martin, R.; Barenhoff, K.; Duponchel, S.; Heider, D.; Fischer, M.G. Four High-Quality Draft Genome Assemblies of the Marine Heterotrophic Nanoflagellate Cafeteria roenbergensis. *Sci. Data* **2020**, *7*, 29. [[CrossRef](#)] [[PubMed](#)]
102. Colatriano, D.; Tran, P.Q.; Guéguen, C.; Williams, W.J.; Lovejoy, C.; Walsh, D.A. Genomic Evidence for the Degradation of Terrestrial Organic Matter by Pelagic Arctic Ocean Chloroflexi Bacteria. *Commun. Biol.* **2018**, *1*, 90. [[CrossRef](#)] [[PubMed](#)]
103. Desnues, C.; Scola, B.L.; Yutin, N.; Fournous, G.; Robert, C.; Azza, S.; Jardot, P.; Monteil, S.; Campocasso, A.; Koonin, E.V.; et al. Provirophages and Transpovirons as the Diverse Mobilome of Giant Viruses. *Proc. Natl. Acad. Sci. USA* **2012**, *109*, 18078–18083. [[CrossRef](#)]
104. Tallada, S.; Hall, G.; Barich, D.; Morgan-Kiss, R.M.; Slonczewski, J.L. Antibiotic Resistance Genes and Taxa Analysis from Mat and Planktonic Microbiomes of Antarctic Perennial Ice-Covered Lake Fryxell and Lake Bonney. *Antarct. Sci.* **2021**, *34*, 408–422. [[CrossRef](#)]
105. Kantor, R.S.; van Zyl, A.W.; van Hille, R.P.; Thomas, B.C.; Harrison, S.T.L.; Banfield, J.F. Bioreactor Microbial Ecosystems for Thiocyanate and Cyanide Degradation Unravelling with Genome-Resolved Metagenomics: Metagenomics of Thiocyanate/Cyanide Biodegradation. *Environ. Microbiol.* **2015**, *17*, 4929–4941. [[CrossRef](#)]
106. Tran, P.; Ramachandran, A.; Khawasik, O.; Beisner, B.E.; Rautio, M.; Huot, Y.; Walsh, D.A. Microbial Life under Ice: Metagenome Diversity and in Situ Activity of Verrucomicrobia in Seasonally Ice-covered Lakes. *Environ. Microbiol.* **2018**, *20*, 2568–2584. [[CrossRef](#)]
107. Rodriguez-R, L.M.; Tsementzi, D.; Luo, C.; Konstantinidis, K.T. Iterative Subtractive Binning of Freshwater Chronoserries Metagenomes Identifies over 400 Novel Species and Their Ecologic Preferences. *Environ. Microbiol.* **2020**, *22*, 3394–3412. [[CrossRef](#)] [[PubMed](#)]

108. Michaud, C.; Hervé, V.; Dupont, S.; Dubreuil, G.; Bézier, A.M.; Meunier, J.; Brune, A.; Dedeine, F. Efficient but Occasionally Imperfect Vertical Transmission of Gut Mutualistic Protists in a Wood-Feeding Termite. *Mol. Ecol.* **2020**, *29*, 308–324. [[CrossRef](#)] [[PubMed](#)]
109. Hess, M.; Sczyrba, A.; Egan, R.; Kim, T.-W.; Chokhawala, H.; Schroth, G.; Luo, S.; Clark, D.S.; Chen, F.; Zhang, T.; et al. Metagenomic Discovery of Biomass-Degrading Genes and Genomes from Cow Rumen. *Science* **2011**, *331*, 463–467. [[CrossRef](#)]
110. Schulz, F.; Yutin, N.; Ivanova, N.N.; Ortega, D.R.; Lee, T.K.; Vierheilig, J.; Daims, H.; Horn, M.; Wagner, M.; Jensen, G.J.; et al. Giant Viruses with an Expanded Complement of Translation System Components. *Science* **2017**, *85*, 82–85. [[CrossRef](#)]
111. Maresca, J.A.; Miller, K.J.; Keffer, J.L.; Sabanayagam, C.R.; Campbell, B.J. Distribution and Diversity of Rhodopsin-Producing Microbes in the Chesapeake Bay. *Appl. Environ. Microbiol.* **2018**, *84*, e00137-18. [[CrossRef](#)] [[PubMed](#)]
112. Props, R.; Deneff, V.J. Temperature and Nutrient Levels Correspond with Lineage-Specific Microdiversification in the Ubiquitous and Abundant Freshwater Genus *Limnohabitans*. *Appl. Environ. Microbiol.* **2020**, *86*, e00140-20. [[CrossRef](#)]
113. Xu, S.; Zhou, L.; Liang, X.; Zhou, Y.; Chen, H.; Yan, S.; Wang, Y.; Science, M.; Biology, M.C. Novel Cell-Virus-Virophage Tripartite Infection Systems Discovered in the Freshwater Lake Dishui Lake in Shanghai, China. *J. Virol.* **2020**, *94*, e00149-20. [[CrossRef](#)]
114. He, S.; Malfatti, S.A.; McFarland, J.W.; Anderson, F.E.; Pati, A.; Huntemann, M.; Tremblay, J.; Glavina del Rio, T.; Waldrop, M.P.; Windham-Myers, L.; et al. Patterns in Wetland Microbial Community Composition and Functional Gene Repertoire Associated with Methane Emissions. *mBio* **2015**, *6*, e00066-15. [[CrossRef](#)]
115. Podowski, J.C.; Paver, S.F.; Newton, R.J.; Coleman, M.L. Genome Streamlining, Proteorhodopsin, and Organic Nitrogen Metabolism in Freshwater Nitrifiers. *mBio* **2022**, *13*, e02379-21. [[CrossRef](#)]
116. Koltun, M.; Weston, D.J.; Mayali, X.; Weber, P.K.; McFarlane, K.J.; Pett-Ridge, J.; Somoza, M.M.; Lietard, J.; Glass, J.B.; Lilleskov, E.A.; et al. Defining the *Sphagnum* Core Microbiome across the North American Continent Reveals a Central Role for Diazotrophic Methanotrophs in the Nitrogen and Carbon Cycles of Boreal Peatland Ecosystems. *mBio* **2022**, *13*, e03714-21. [[CrossRef](#)]
117. Garcia, S.L.; Buck, M.; Hamilton, J.J.; Wurzbacher, C.; Grossart, H.-P.; McMahon, K.D.; Eiler, A. Model Communities Hint at Promiscuous Metabolic Linkages between Ubiquitous Free-Living Freshwater Bacteria. *mSphere* **2018**, *3*, e00202-18. [[CrossRef](#)] [[PubMed](#)]
118. Zhou, Z.; Liu, Y.; Xu, W.; Pan, J.; Luo, Z.-H.; Li, M. Genome- and Community-Level Interaction Insights into Carbon Utilization and Element Cycling Functions of *Hydrothermarchaeota* in Hydrothermal Sediment. *mSystems* **2020**, *5*, e00795-19. [[CrossRef](#)] [[PubMed](#)]
119. Sun, M.; Zhan, Y.; Marsan, D.; Páez-Espino, D.; Cai, L.; Chen, F. Uncultivated Viral Populations Dominate Estuarine Viromes on the Spatiotemporal Scale. *mSystems* **2021**, *6*, e01020-20. [[CrossRef](#)] [[PubMed](#)]
120. Baker, B.J.; Lazar, C.S.; Teske, A.P.; Dick, G.J. Genomic Resolution of Linkages in Carbon, Nitrogen, and Sulfur Cycling among Widespread Estuary Sediment Bacteria. *Microbiome* **2015**, *3*, 14. [[CrossRef](#)]
121. Tschitschko, B.; Erdmann, S.; DeMaere, M.Z.; Roux, S.; Panwar, P.; Allen, M.A.; Williams, T.J.; Brazendale, S.; Hancock, A.M.; Eloe-Fadrosh, E.A.; et al. Genomic Variation and Biogeography of Antarctic Haloarchaea. *Microbiome* **2018**, *6*, 113. [[CrossRef](#)]
122. Martins, P.D.; Danczak, R.E.; Roux, S.; Frank, J.; Borton, M.A.; Wolfe, R.A.; Burris, M.N.; Wilkins, M.J. Viral and Metabolic Controls on High Rates of Microbial Sulfur and Carbon Cycling in Wetland Ecosystems. *Microbiome* **2018**, *6*, 138. [[CrossRef](#)]
123. Panwar, P.; Allen, M.A.; Williams, T.J.; Hancock, A.M.; Brazendale, S.; Bevington, J.; Roux, S.; Páez-Espino, D.; Nayfach, S.; Berg, M.; et al. Influence of the Polar Light Cycle on Seasonal Dynamics of an Antarctic Lake Microbial Community. *Microbiome* **2020**, *8*, 116. [[CrossRef](#)]
124. ter Horst, A.M.; Santos-Medellín, C.; Sorensen, J.W.; Zinke, L.A.; Wilson, R.M.; Johnston, E.R.; Trubl, G.G.; Pett-Ridge, J.; Blazewicz, S.J.; Hanson, P.J.; et al. Minnesota Peat Viromes Reveal Terrestrial and Aquatic Niche Partitioning for Local and Global Viral Populations. *Microbiome* **2021**, *9*, 233. [[CrossRef](#)]
125. Amundson, K.K.; Borton, M.A.; Daly, R.A.; Hoyt, D.W.; Wong, A.; Eder, E.; Moore, J.; Wunch, K.; Wrighton, K.C.; Wilkins, M.J. Microbial Colonization and Persistence in Deep Fractured Shales Is Guided by Metabolic Exchanges and Viral Predation. *Microbiome* **2022**, *10*, 5. [[CrossRef](#)]
126. Duncan, A.; Barry, K.; Daum, C.; Eloe-Fadrosh, E.; Roux, S.; Schmidt, K.; Tringe, S.G.; Valentin, K.U.; Varghese, N.; Salamov, A.; et al. Metagenome-Assembled Genomes of Phytoplankton Microbiomes from the Arctic and Atlantic Oceans. *Microbiome* **2022**, *10*, 67. [[CrossRef](#)]
127. Abraham, B.S.; Caglayan, D.; Carrillo, N.V.; Chapman, M.C.; Hagan, C.T.; Hansen, S.T.; Jeanty, R.O.; Klimczak, A.A.; Klingler, M.J.; Kutcher, T.P.; et al. Shotgun Metagenomic Analysis of Microbial Communities from the Loxahatchee Nature Preserve in the Florida Everglades. *Environ. Microbiome* **2020**, *15*, 2. [[CrossRef](#)] [[PubMed](#)]
128. Gaia, M.; Pagnier, I.; Campocasso, A.; Fournous, G.; Raoult, D.; La Scola, B. Broad Spectrum of Mimiviridae Virophage Allows Its Isolation Using a Mimivirus Reporter. *PLoS ONE* **2013**, *8*, e61912. [[CrossRef](#)] [[PubMed](#)]
129. Hubbard, S.S.; Williams, K.H.; Agarwal, D.; Banfield, J.; Beller, H.; Bouskill, N.; Brodie, E.; Carroll, R.; Dafflon, B.; Dwivedi, D.; et al. The East River, Colorado, Watershed: A Mountainous Community Testbed for Improving Predictive Understanding of Multiscale Hydrological–Biogeochemical Dynamics. *Vadose Zone J.* **2018**, *17*, 1–25. [[CrossRef](#)]
130. Kelly, C. *Quantifying Ecosystem Changes Following American Chestnut Restoration: From Microbes to Ecosystem Function*; DOE Joint Genome Institute: Berkeley, CA, USA, 2017. [[CrossRef](#)]

131. Davenport, E.J.; Neudeck, M.J.; Matson, P.G.; Bullerjahn, G.S.; Davis, T.W.; Wilhelm, S.W.; Denney, M.K.; Krausfeldt, L.E.; Stough, J.M.A.; Meyer, K.A.; et al. Metatranscriptomic Analyses of Diel Metabolic Functions During a Microcystis Bloom in Western Lake Erie (United States). *Front. Microbiol.* **2019**, *10*, 2081. [[CrossRef](#)] [[PubMed](#)]
132. Garcia, M.O.; Templer, P.H.; Sorensen, P.O.; Sanders-DeMott, R.; Groffman, P.M.; Bhatnagar, J.M. Soil Microbes Trade-Off Biogeochemical Cycling for Stress Tolerance Traits in Response to Year-Round Climate Change. *Front. Microbiol.* **2020**, *11*, 616. [[CrossRef](#)]
133. Figueroa-Gonzalez, P.A.; Bornemann, T.L.V.; Adam, P.S.; Plewka, J.; Révész, F.; von Hagen, C.A.; Táncsics, A.; Probst, A.J. Saccharibacteria as Organic Carbon Sinks in Hydrocarbon-Fueled Communities. *Front. Microbiol.* **2020**, *11*, 587782. [[CrossRef](#)]
134. Williams, T.J.; Allen, M.A.; Ivanova, N.; Huntemann, M.; Haque, S.; Hancock, A.M.; Brazendale, S.; Cavicchioli, R. Genome Analysis of a Verrucomicrobial Endosymbiont With a Tiny Genome Discovered in an Antarctic Lake. *Front. Microbiol.* **2021**, *12*, 674758. [[CrossRef](#)]
135. Linz, A.M.; He, S.; Stevens, S.L.R.; Anantharaman, K.; Rohwer, R.R.; Malmstrom, R.R.; Bertilsson, S.; McMahon, K.D. Freshwater Carbon and Nutrient Cycles Revealed through Reconstructed Population Genomes. *PeerJ* **2018**, *6*, e6075. [[CrossRef](#)]

**Disclaimer/Publisher's Note:** The statements, opinions and data contained in all publications are solely those of the individual author(s) and contributor(s) and not of MDPI and/or the editor(s). MDPI and/or the editor(s) disclaim responsibility for any injury to people or property resulting from any ideas, methods, instructions or products referred to in the content.